

Radiative Corrections to the $Zb\bar{b}$ Vertex and Constraints on Extended Higgs Sectors

Howard E. Haber and Heather E. Logan

*Santa Cruz Institute for Particle Physics
University of California, Santa Cruz, CA 95064, U.S.A.*

Abstract

We explore the radiative corrections to the process $Z \rightarrow b\bar{b}$ in models with extended Higgs sectors. The observables $R_b \equiv \Gamma(Z \rightarrow b\bar{b})/\Gamma(Z \rightarrow \text{hadrons})$ and the $Zb\bar{b}$ coupling asymmetry, $A_b \equiv (g_L^2 - g_R^2)/(g_L^2 + g_R^2)$, are sensitive to these corrections. We present general formulae for the one-loop corrections to R_b and A_b in an arbitrary extended Higgs sector, and derive explicit results for a number of specific models. We find that in models containing only doublets, singlets, or larger multiplets constrained by a custodial $SU(2)_c$ symmetry so that $M_W = M_Z \cos \theta_W$ at tree level, the one-loop corrections due to virtual charged Higgs bosons always worsen agreement with experiment. The R_b measurement can be used to set lower bounds on the charged Higgs masses. Constraints on models due to the one-loop contributions of neutral Higgs bosons are also examined.

1 Introduction

The Standard Model of electroweak interactions has been tested to unprecedented precision during the past decade at the LEP and SLC colliders [1,2,3]. Global fits of electroweak observables have confirmed that the electroweak interactions are well described by a spontaneously broken $SU(2) \times U(1)$ gauge theory. However, these measurements have not yet revealed the underlying dynamics responsible for electroweak symmetry breaking (EWSB).

In the Standard Model (SM), the electroweak symmetry is broken by the dynamics of a weakly coupled scalar Higgs sector consisting of one complex $SU(2)$ doublet of scalar fields with hypercharge $Y = 1$. After EWSB, three scalar degrees of freedom (Goldstone bosons) are absorbed by the W and Z , leaving one CP-even neutral Higgs boson H^0 in the physical spectrum. The SM Higgs sector possesses an unbroken global $SU(2)$ symmetry of the EWSB sector, often called “custodial $SU(2)$ symmetry” [4]. This symmetry leads to the tree-level relation, $\rho \equiv M_W^2/M_Z^2 \cos^2 \theta_W = 1$, a relation that is satisfied experimentally to better than a few parts in a thousand [5].

Precision electroweak data is now accurate enough to provide non-trivial tests of the one-loop structure of the SM. In particular, one can begin to test the EWSB sector of the theory by probing the one-loop virtual effects of the Higgs sector. The couplings of Higgs bosons to fermions and gauge bosons are proportional to the fermion and gauge boson masses, respectively. As a result, one-loop corrections involving Higgs bosons coupled to W , Z or third-generation quarks can be significant. In the SM, loop corrections involving H^0 coupling to gauge bosons depend logarithmically on the H^0 mass. A fit to the electroweak data gives an upper bound on the SM Higgs mass of $M_{h^0} \lesssim 220$ GeV at the 95% confidence level [1,3]. In the SM, the Higgs couplings to third-generation quarks do not provide additional constraints on the Higgs sector. Virtual Higgs exchange does contribute to the decay $Z \rightarrow b\bar{b}$; however, the coupling of H^0 to b -quarks is too small to make an observable contribution. The coupling of the charged Goldstone bosons G^\pm to $t\bar{b}$ is large enough to make an observable contribution to $Z \rightarrow b\bar{b}$, but this contribution is fixed by electroweak symmetry; it depends only on the W and t -quark masses, the electromagnetic coupling and $\sin^2 \theta_W$ [6,7,8,9,10].

Many extensions to the minimal SM Higgs sector are possible. (For a comprehensive review, see ref. [11].) As in the SM, extended models typically must contain at least one complex $Y = 1$ $SU(2)$ doublet in order to give mass to the fermions. Additional $SU(2)$ doublets, singlets, and/or larger multiplets may also be present. Such extended Higgs sectors contain charged Higgs bosons and/or additional neutral Higgs bosons in the physical spectrum. Some constraints on the model exist due to the observed $\rho \simeq 1$; this can restrict the choices of Higgs multiplets or require a fine-tuning of the vacuum expectation values of the neutral Higgs

fields. In addition, the experimentally observed suppression of flavor changing neutral currents (FCNC's) implies that Higgs-mediated tree-level FCNC's are either absent (which constrains the Higgs-fermion couplings of the model [12,13]), or suppressed [14]. In the latter case, the suppression of FCNC's can be achieved if the non-minimal Higgs states are sufficiently heavy (thereby approximately decoupling from the sector of SM particles [15]).

Extended Higgs sectors also contribute virtually to one-loop processes involving SM particles. In this paper our primary focus concerns the electroweak observables associated with $Z \rightarrow b\bar{b}$. In this case, the Higgs sector can yield observable corrections at one-loop through charged Higgs couplings to $t\bar{b}$ and the neutral Higgs couplings to $b\bar{b}$. These can then provide new constraints on the possible structure of the non-minimal Higgs sector.

The process $Z \rightarrow b\bar{b}$ yields two observable quantities, R_b and A_b . R_b is the hadronic branching ratio of Z to b quarks,

$$R_b \equiv \frac{\Gamma(Z \rightarrow b\bar{b})}{\Gamma(Z \rightarrow \text{hadrons})}, \quad (1.1)$$

and A_b is the b -quark asymmetry,

$$A_b = \frac{\sigma(e_L^- \rightarrow b_F) - \sigma(e_L^- \rightarrow b_B) + \sigma(e_R^- \rightarrow b_B) - \sigma(e_R^- \rightarrow b_F)}{\sigma(e_L^- \rightarrow b_F) + \sigma(e_L^- \rightarrow b_B) + \sigma(e_R^- \rightarrow b_B) + \sigma(e_R^- \rightarrow b_F)}, \quad (1.2)$$

where $e_{L,R}^-$ are left and right handed initial-state electrons and $b_{F,B}$ are final-state b -quarks moving in the forward and backward directions with respect to the direction of the initial-state electrons. In terms of the b -quark couplings to Z ,

$$A_b = \frac{(g_{Zb\bar{b}}^L)^2 - (g_{Zb\bar{b}}^R)^2}{(g_{Zb\bar{b}}^L)^2 + (g_{Zb\bar{b}}^R)^2}. \quad (1.3)$$

In this paper we introduce a parameterization for a general extended Higgs sector and calculate the contribution to $Z \rightarrow b\bar{b}$ from one-loop radiative corrections involving singly charged and neutral Higgs bosons. We obtain general expressions for the corrections to the left- and right-handed $Zb\bar{b}$ couplings, and then use the measurements of R_b and A_b to constrain specific models. This approach has the advantage of yielding general formulae for the corrections in terms of the couplings and masses of the Higgs bosons. The formulae can then be specialized to any extended Higgs model by inserting the appropriate couplings. Kundu and Mukhopadhyaya [16] have taken the same approach and calculated the charged Higgs boson contributions to $Z \rightarrow b\bar{b}$ in a general extended Higgs sector. However, the neutral Higgs boson contributions in a general extended Higgs sector do not appear in the literature. Specific results for the one-loop corrections to $Z \rightarrow b\bar{b}$ in two-Higgs-doublet models (2HDM's) can be found in refs. [17,18,19,20].

One-loop corrections to $Z \rightarrow b\bar{b}$ can also arise from other sources of new physics. Thus, any derivation of constraints on the Higgs sector based on the effects of Higgs virtual corrections must assume that these are the dominant (or only) source of corrections beyond the Standard Model. For example, in theories of low-energy supersymmetry, it is easy to find ranges of parameter space in which the effects of virtual supersymmetric particle exchange compete (and sometimes cancel out [21]) the effects of virtual Higgs exchange. However, in the limit of large superpartner masses, the supersymmetric contributions decouple [22,23], and the formulae obtained in this paper are once again applicable.

This paper is organized as follows. In section 2 we discuss the measurements of R_b and A_b and the constraints that they put on the $Zb\bar{b}$ couplings. In section 3 we introduce the two Higgs doublet model and then generalize to an arbitrary extended Higgs sector. We then compute the radiative corrections to the $Zb\bar{b}$ coupling due to the virtual exchange of charged Higgs bosons (section 4) and neutral Higgs bosons (section 5), respectively. In section 6 we apply the general formulae for loop corrections to a number of specific models. Based on the current experimental measurements of R_b and A_b , we exhibit the constraints on the parameters of the extended Higgs sector. We first consider extended Higgs sectors containing only doublets and singlets, and then extend the analysis to Higgs sectors which containing larger multiplets in addition to doublets. Finally, we summarize our conclusions in section 7. Additional details can be found in ref. [24].

2 Constraints from the data

The radiative corrections to $Z \rightarrow b\bar{b}$ modify the $Zb\bar{b}$ couplings from their tree-level values. In this section we show how the experimental constraints on R_b and A_b constrain the possible values of the effective $Zb\bar{b}$ couplings. We employ the following notation for the effective $Zb\bar{b}$ interaction:

$$\begin{aligned}\mathcal{L}_{Zb\bar{b}} &= \frac{-e}{2s_W c_W} Z_\mu \bar{b} \gamma^\mu \left[\bar{g}_b^L (1 - \gamma_5) + \bar{g}_b^R (1 + \gamma_5) \right] b \\ &= \frac{-e}{2s_W c_W} Z_\mu \bar{b} \gamma^\mu (\bar{v}_b - \bar{a}_b \gamma_5) b,\end{aligned}\tag{2.1}$$

where $s_W \equiv \sin \theta_W$ and $c_W \equiv \cos \theta_W$. The effective couplings are then written as

$$\bar{g}_b^{L,R} = g_{Zb\bar{b}}^{L,R} + \delta g^{L,R},\tag{2.2}$$

where $\bar{g}_b^{L,R}$ are the radiatively-corrected effective couplings, and the tree-level couplings are given by $g_{Zb\bar{b}}^L \equiv -\frac{1}{2} + \frac{1}{3}s_W^2$ and $g_{Zb\bar{b}}^R \equiv \frac{1}{3}s_W^2$.

2.1 Extracting the effective $Zb\bar{b}$ couplings from R_b and A_b

Following the discussion by Field [25] and using his notation, the effective couplings $\bar{g}_b^{L,R}$ are related to R_b and A_b as follows.

$$R_b = \left[1 + \frac{S_b}{\bar{s}_b C_b^{QCD} C_b^{QED}} \right]^{-1},$$

$$A_b = \frac{2\bar{r}_b(1 - 4\mu_b)^{1/2}}{1 - 4\mu_b + (1 + 2\mu_b)\bar{r}_b^2}, \quad (2.3)$$

where C_b^{QCD} and C_b^{QED} are QCD and QED radiative correction factors. Using $\alpha_s(M_Z) = 0.12$ and $\alpha^{-1}(M_Z) = 128.9$, the numerical values of these factors are: $C_b^{QCD} = 0.9953$ and $C_b^{QED} = 0.99975$. In addition,

$$\bar{r}_b \equiv \frac{\bar{v}_b}{\bar{a}_b},$$

$$\bar{s}_b \equiv (\bar{a}_b)^2(1 - 6\mu_b) + (\bar{v}_b)^2,$$

$$S_b \equiv \sum_{q \neq b,t} [(\bar{a}_q)^2 + (\bar{v}_q)^2],$$

$$\mu_b \equiv [m_b(M_Z)/M_Z]^2. \quad (2.4)$$

In the definition of S_b , the sum is taken only over first and second generation quarks. To a good approximation, we can neglect the contributions of new physics to S_b , and fix this quantity to its SM predicted value. Using the corresponding SM predicted values: $\bar{v}_u = 0.1916$, $\bar{a}_u = 0.5012$, $\bar{v}_d = -0.3464$ and $\bar{a}_d = -0.5012$ for the vector and axial couplings of the first and second generation up-type and down-type quarks taken from ref. [25], we obtain $S_b = 1.3184$. The b -quark contribution is separated out in the quantity \bar{s}_b ; here μ_b is a correction factor coming from the nonzero b -quark mass. This correction factor is roughly $\mu_b \simeq 1.0 \times 10^{-3}$, where we have taken the running b -quark mass in the $\overline{\text{MS}}$ scheme evaluated at M_Z , $m_b(M_Z) = 3.0$ GeV [26].

We can solve the above equations for \bar{g}_b^L and \bar{g}_b^R in terms of the experimentally measured values for R_b and A_b . Using the predicted SM values given in ref. [25]:

$$(\bar{g}_b^L)_{\text{SM}} = -0.4208, \quad (\bar{g}_b^R)_{\text{SM}} = 0.0774, \quad (2.5)$$

we obtain the SM predictions for R_b and A_b :

$$R_b^{\text{SM}} = 0.2158, \quad (2.6)$$

$$A_b^{\text{SM}} = 0.935. \quad (2.7)$$

These results should be compared with the measured values [2]

$$R_b = 0.21642 \pm 0.00073, \quad (2.8)$$

$$A_b = 0.893 \pm 0.016. \quad (2.9)$$

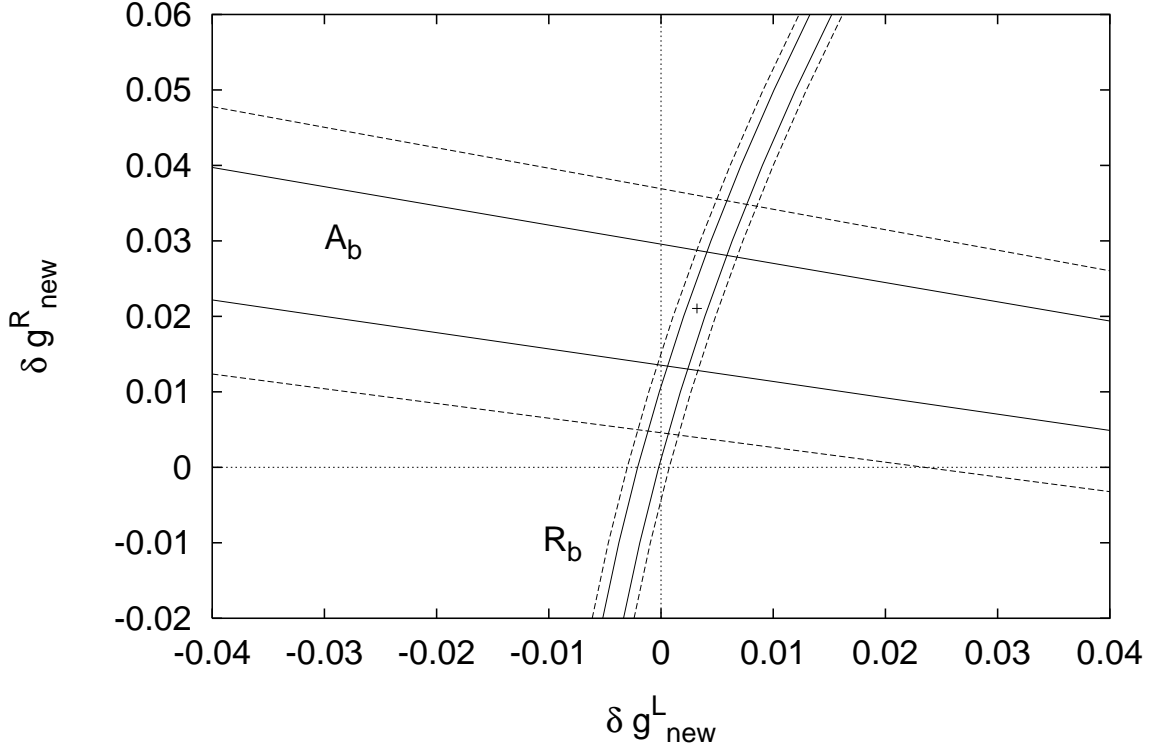


Fig. 1. The constraints from R_b and A_b on the right- and left-handed $Zb\bar{b}$ couplings. Plotted are the allowed deviations $\delta g_{\text{new}}^{R,L}$ of the couplings from their SM values. The 1σ errors are shown as solid lines and the 2σ errors as dashed lines. The central value, at $\delta g_{\text{new}}^L = 0.0037$ and $\delta g_{\text{new}}^R = 0.0219$, is marked by the cross.

R_b is measured directly at LEP and SLD. A_b is measured directly at SLD from the left-right forward-backward asymmetry, and indirectly at LEP from the measured value of A_e and the forward-backward asymmetry $A_{FB}^{0,b} = \frac{3}{4}A_e A_b$. The R_b measurement is 0.8σ above the SM prediction, and the A_b measurement is 2.6σ below the SM prediction.

Allowing for a deviation of the experimentally measured values of $\bar{g}_b^{L,R}$ from their predicted values in the SM, we write:

$$\left(\bar{g}_b^{L,R}\right)_{\text{expt}} = \left(\bar{g}_b^{L,R}\right)_{\text{SM}} + \delta g_{\text{new}}^{L,R}. \quad (2.10)$$

The experimental constraints from R_b and A_b on $\delta g_{\text{new}}^{L,R}$ are shown in fig. 1. The central value is at $\delta g_{\text{new}}^L = 0.0037$ and $\delta g_{\text{new}}^R = 0.0219$. Comparing these to the SM predictions, we see that δg_{new}^L is roughly a 1% correction while δg_{new}^R is close to a 30% correction.

It is also useful to expand R_b and A_b about their SM values, to first order in

$\delta g_{\text{new}}^{L,R}$. Using the SM parameters given above, we find

$$\begin{aligned}\delta R_b &= -0.7785 \delta g_{\text{new}}^L + 0.1409 \delta g_{\text{new}}^R, \\ \delta A_b &= -0.2984 \delta g_{\text{new}}^L - 1.6234 \delta g_{\text{new}}^R.\end{aligned}\tag{2.11}$$

Note that a positive δg_{new}^L decreases both R_b and A_b , while a positive δg_{new}^R increases R_b and decreases A_b . Inverting the above results yields

$$\begin{aligned}\delta g_{\text{new}}^L &= -1.2433 \delta R_b - 0.1079 \delta A_b, \\ \delta g_{\text{new}}^R &= 0.2286 \delta R_b - 0.5962 \delta A_b.\end{aligned}\tag{2.12}$$

In practice, these first order results provide a fairly good estimate of δg_{new}^L , and a less reliable estimate of δg_{new}^R . This is easily understood; because the data suggest a rather large relative shift of \bar{g}_b^R from its SM predicted value, second order effects cannot be neglected. In this paper, the more precise analysis based on fig. 1 is used in our analysis of new physics contributions to R_b and A_b from extended Higgs sectors.¹

2.2 Tree-level $Zb\bar{b}$ couplings: The effect of oblique corrections

In the SM, all electroweak observables are fixed by the measurement of three quantities, commonly chosen to be the electromagnetic fine structure constant α , the muon decay constant G_μ , and the Z mass. In particular, by measuring these quantities, one can predict the value of $\sin^2 \theta_{\text{eff}}^{\text{lept}}$. In practice, many more electroweak observables are measured and a fit is made to the SM parameters (see *e.g.*, ref. [27]).

However, the dependence of $\sin^2 \theta_{\text{eff}}^{\text{lept}}$ on other electroweak observables can be modified in models of physics beyond the SM. The dominant effect of the new physics (in most cases) enters via the virtual loop corrections to gauge boson self-energies; these are the oblique corrections. These modifications are parameterized by the Peskin–Takeuchi parameters S , T , and U [28]. In particular [29],

$$\begin{aligned}\sin^2 \theta_{\text{eff}}^{\text{lept}} - [\sin^2 \theta_{\text{eff}}^{\text{lept}}]_{\text{SM}} &\equiv \delta s_W^2 = \frac{\alpha}{c_W^2 - s_W^2} \left[\frac{1}{4} S - s_W^2 c_W^2 T \right] \\ &= 3.40 \times 10^{-3} S - 2.42 \times 10^{-3} T,\end{aligned}\tag{2.13}$$

where we have used $s_W^2 \equiv [\sin^2 \theta_{\text{eff}}^{\text{lept}}]_{\text{SM}} = 0.231$. Nonzero values of the S and T parameters therefore modify the prediction for the tree-level $Zb\bar{b}$ couplings $g_{Zb\bar{b}}^{L,R}$.

¹The bounds on Higgs sector parameters obtained in section 6 are based on a slightly older analysis of electroweak data presented in ref. [1], which reported a slightly higher value of R_b and A_b . The effect of the updated numbers on our plots is not significant and does not alter our general conclusions.

The S , T and U parameters are defined relative to a reference SM, with a fixed Higgs mass. For $M_{h^0} = M_Z$, a fit of the electroweak data gives [30]

$$\begin{aligned} S &= -0.16 \pm 0.14, \\ T &= -0.21 \pm 0.16, \\ U &= 0.25 \pm 0.24. \end{aligned} \tag{2.14}$$

This analysis has not yet been updated to account for the latest available precision electroweak data. However, for our purposes, it is sufficient to note is that the fitted absolute values of S and T are significantly less than $\mathcal{O}(1)$.

In order to understand the significance of oblique corrections of this size, we compute the corrections to the predictions for R_b and A_b due to S and T (there is no U dependence). To first order in δs_W^2 , eq. (2.10) is modified to

$$\left(\bar{g}_b^{L,R}\right)_{\text{expt}} = \left(\bar{g}_b^{L,R}\right)_{\text{SM}} + \delta g_{\text{new}}^{L,R} + \frac{1}{3}\delta s_W^2. \tag{2.15}$$

The last term is simply a consequence of the form of the $Zb\bar{b}$ tree-level couplings. Since A_b depends only on $\bar{g}_b^{L,R}$, one may simply combine the results of eqs. (2.11), (2.13) and (2.15) to obtain:

$$\delta A_b = -0.641\delta s_W^2 = -2.18 \times 10^{-3} S + 1.55 \times 10^{-3} T. \tag{2.16}$$

To obtain δR_b , one must also account for the effect of the oblique corrections on $g_u^{L,R}$ and $g_d^{L,R}$ which enter in the expression for $\Gamma(Z \rightarrow \text{hadrons})$. Following ref. [29], we find:

$$\delta R_b = 0.0388\delta s_W^2 = 1.32 \times 10^{-4} S - 0.94 \times 10^{-4} T. \tag{2.17}$$

For values of S and T significantly less than $\mathcal{O}(1)$, the shift in the predicted value of R_b and A_b due to nonzero values of S and T is less than a few percent of the present experimental error on both R_b and A_b . We can therefore safely neglect these corrections.

3 Models with extended Higgs sectors

A wide variety of extensions to the minimal SM Higgs sector are possible [11]. We assume that the Higgs sector contains at least one complex $\text{SU}(2)_L$ doublet with $Y = 1$ to give mass to the SM fermions. In our notation, ϕ_k denotes a multiplet of scalar fields that transforms as a complex representation under $\text{SU}(2) \times \text{U}(1)$.²

²Given a complex Higgs multiplet, Φ , with $Y \neq 0$, one can always construct the complex conjugated multiplet, Φ^* , with hypercharge $-Y$. Henceforth, without loss of generality, we shall focus only on Higgs multiplets with $Y \geq 0$.

A real representation (*i.e.*, a real multiplet of fields with integer weak isospin and hypercharge $Y = 0$) is denoted by η_i . For simplicity, we assume that the Higgs sector is CP-conserving, so that the neutral Higgs mass eigenstates are either CP-even (H_i^0) or CP-odd (A_j^0). The Higgs potential is chosen to break $SU(2)_L \times U(1)_Y$ down to $U(1)_{EM}$. That is, we assume that only the neutral member of each Higgs multiplet can acquire a non-zero vacuum expectation value (vev). For the neutral scalar component of a complex representation, the vev is normalized such that

$$\phi_k^0 \equiv \sqrt{\frac{1}{2}} \left(v_k + \phi_k^{0,r} + i\phi_k^{0,i} \right), \quad (3.1)$$

where $\langle \phi_k^0 \rangle = v_k/\sqrt{2}$. For real representations, we take $\langle \eta_i^0 \rangle = v_i$.

Given the Higgs representations and the vevs, the Goldstone bosons eigenstates are determined. The neutral Goldstone boson is given by

$$G^0 = \left[\sum_k v_k^2 Y_k^2 \right]^{-1/2} \sum_k v_k^2 Y_k^2 \phi_k^{0,i}, \quad (3.2)$$

and the positively charged Goldstone boson is given by

$$G^+ = N^{-1} \left[\sum_k \left\{ \left[T_k(T_k + 1) - \frac{1}{4} Y_k(Y_k - 2) \right]^{1/2} v_k \phi_k^+ - \left[T_k(T_k + 1) - \frac{1}{4} Y_k(Y_k + 2) \right]^{1/2} v_k (\phi_k^-)^* \right\} + \sum_i [2T_i(T_i + 1)]^{1/2} v_i \eta_i^+ \right], \quad (3.3)$$

where the normalization factor is given by

$$N^2 \equiv \sum_k 2v_k^2 \left[T_k(T_k + 1) - \frac{1}{4} Y_k^2 \right] + \sum_i 2v_i^2 T_i(T_i + 1). \quad (3.4)$$

In the above equations, we have separated out the sums into contributions from the complex Higgs representations k and the real Higgs representations i . Note that for a Higgs boson in a complex representation, $(\phi^Q)^*$ is a state with charge $-Q$ but is not the same as ϕ^{-Q} . For a Higgs boson in a real representation, we adopt the phase convention such that $(\eta^+)^* = -\eta^-$. Thus, in our phase convention, the negatively charged Goldstone boson is given by $G^- = -(G^+)^*$.

Since we wish to preserve $U(1)_{EM}$, we assume that only neutral Higgs fields acquire vevs. These Higgs vevs are constrained by the W mass, which for a general extended Higgs sector is given by

$$M_W^2 = \frac{1}{4} g^2 N^2 = \frac{1}{4} g^2 v_{SM}^2, \quad (3.5)$$

where N^2 is given by eq. (3.4). Thus, we can identify $N \equiv v_{SM} = 246$ GeV.

The vevs and/or the Higgs representation content are also constrained by the ρ -parameter, which at tree-level is given by [11]

$$\rho \equiv \frac{m_W^2}{M_Z^2 c_W^2} = \frac{N^2}{\sum_k v_k^2 Y_k^2}. \quad (3.6)$$

The observed electroweak data imply that the tree-level value of ρ must be very close to (or perhaps exactly equal to) unity.

In a Higgs sector that contains only multiplets which satisfy the relation

$$(2T + 1)^2 - 3Y^2 = 1, \quad (3.7)$$

one finds $\rho = 1$ at tree level for any combination of vevs. Eq. (3.7) is satisfied, for example, by the familiar Higgs doublet with $Y = 1$, and by a series of larger multiplets [31].³ In such a Higgs sector, the formulae for G^+ and M_W^2 simplify to

$$G^+ = \left[\sum_k v_k^2 Y_k^2 \right]^{-1/2} \sum_k \sqrt{\frac{1}{2}} v_k \left[(Y_k^2 + Y_k)^{1/2} \phi_k^+ - (Y_k^2 - Y_k)^{1/2} (\phi_k^-)^* \right], \quad (3.8)$$

and

$$M_W^2 = \frac{1}{4} g^2 \sum_k v_k^2 Y_k^2. \quad (3.9)$$

In the SM, the diagonalization of the quark mass matrix automatically diagonalizes the Yukawa couplings of the neutral Higgs boson to quarks. Thus in the SM, there are no FCNC's mediated by tree-level Higgs exchange. However, in a multi-doublet Higgs sector with the most general Higgs-fermion Yukawa couplings, tree-level Higgs-mediated FCNC's can arise. These can be automatically eliminated in any Higgs model in which fermions of a given electric charge receive their mass from couplings to exactly one neutral Higgs field [12,13]. This pattern of Higgs-fermion couplings can be implemented by a judicious choice of discrete symmetries. There are two possible configurations for the Higgs-quark Yukawa couplings in an extended Higgs sector that contains at least one scalar doublet with $Y = 1$. In Type I models, all the quarks couple to one doublet, Φ_1 . In Type II models, the down-type quarks couple to Φ_1 and the up-type quarks couple to a second $Y = 1$ doublet, Φ_2 . If the general extended Higgs sector contains only one $Y = 1$ doublet, then its Yukawa couplings are necessarily Type I.

In a Type I model, one Higgs doublet Φ_1 gives mass to both t and b quarks. The Yukawa couplings are

$$\lambda_t = \frac{\sqrt{2} m_t}{v_1}, \quad \lambda_b = \frac{\sqrt{2} m_b}{v_1}. \quad (3.10)$$

³Of course, one can always add gauge neutral singlet scalars with arbitrary vevs, without affecting the value of the ρ -parameter.

Note that in a Type I model, $\lambda_b/\lambda_t = m_b/m_t$, so $\lambda_b \ll \lambda_t$ for all values of v_1 .

In a Type II model, Φ_1 couples to b quarks and Φ_2 couples to t quarks. The quark Yukawa couplings are then

$$\lambda_t = \frac{\sqrt{2}m_t}{v_2}, \quad \lambda_b = \frac{\sqrt{2}m_b}{v_1}. \quad (3.11)$$

Note that in a Type II model, $\lambda_b/\lambda_t = (m_b/m_t)(v_2/v_1)$, so λ_b can be enhanced relative to λ_t by choosing $v_1 \ll v_2$.

When the Higgs mass-squared matrix is diagonalized, the electroweak eigenstates mix to form mass eigenstates. The couplings of the Higgs mass eigenstates to quarks take the form

$$i \left(g_{H\bar{q}q}^L P_L + g_{H\bar{q}q}^R P_R \right) = i \left(g_{H\bar{q}q}^V + g_{H\bar{q}q}^A \gamma_5 \right). \quad (3.12)$$

The individual couplings to $b\bar{b}$ and $t\bar{t}$ in a Type II model are given by

$$g_{H_i^0 b\bar{b}}^V = -\frac{\lambda_b}{\sqrt{2}} \langle H_i^0 | \phi_1^{0,r} \rangle, \quad (3.13)$$

$$g_{A_i^0 b\bar{b}}^A = -\frac{i\lambda_b}{\sqrt{2}} \langle A_i^0 | \phi_1^{0,i} \rangle, \quad (3.14)$$

$$g_{H_i^+ t\bar{b}}^R = -\lambda_b \langle H_i^+ | \phi_1^+ \rangle, \quad (3.15)$$

$$g_{H_i^+ t\bar{b}}^L = +\lambda_t \langle H_i^+ | \phi_2^+ \rangle, \quad (3.16)$$

where the bracket notation is used to indicate the overlap between the corresponding mass-eigenstate and interaction-eigenstate. The Type I model couplings are obtained by replacing ϕ_2^+ with ϕ_1^+ in eq. (3.16); the other couplings remain the same.

The Z -Higgs-Higgs couplings take the form $ig_{ZH_1H_2}(p_1 - p_2)^\mu$, where p_1 [p_2] is the incoming momentum of H_1 [H_2]. The Z -Higgs-Higgs couplings involving neutral and singly-charged Higgs bosons are

$$g_{ZH_i^0 A_j^0} = \frac{ie}{s_W c_W} \sum_{k=1}^N \langle H_i^0 | \phi_k^{0,r} \rangle \langle A_j^0 | \phi_k^{0,i} \rangle T_{\phi_k^0}^3, \quad (3.17)$$

$$g_{ZH_i^+ H_j^-} = -\frac{e}{s_W c_W} \left\{ \sum_{k=1}^N \langle H_i^+ | \phi_k^+ \rangle \langle H_j^- | \phi_k^+ \rangle T_{\phi_k^+}^3 - s_W^2 \delta_{ij} \right\}, \quad (3.18)$$

where T_ϕ^3 is the third component of the weak isospin of ϕ . For completeness, we also give the $W^+W^-H_i^0$ and ZZH_i^0 couplings, which take the form $ig_{V_1V_2H}g^{\mu\nu}$. The VVH_i^0 ($V = W^\pm, Z$) couplings are

$$g_{W^+W^-H_i^0} = g^2 \sum_k \langle H_i^0 | \phi_k^{0,r} \rangle v_k \left[T_k(T_k + 1) - \frac{1}{4} Y_k^2 \right], \quad (3.19)$$

$$g_{ZZH_i^0} = \frac{g^2}{2c_W^2} \sum_k \langle H_i^0 | \phi_k^{0,r} \rangle v_k Y_k^2. \quad (3.20)$$

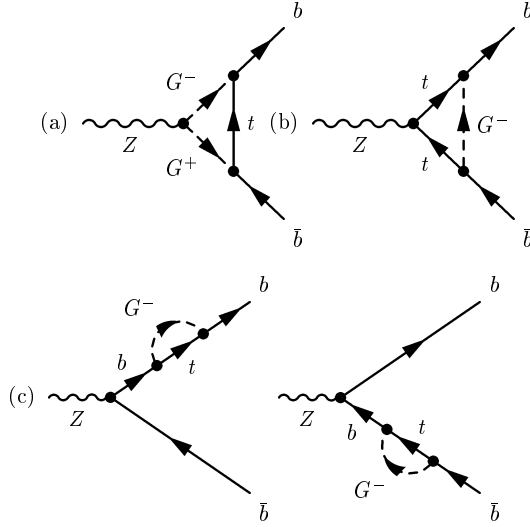


Fig. 2. Feynman diagrams of the leading m_t^2 contributions to the electroweak corrections to $Z \rightarrow b\bar{b}$ in the SM.

A complete list of Higgs–vector boson couplings in a general extended Higgs sector can be found in ref. [24].

Although the Z –Higgs–Higgs couplings are diagonal in the interaction basis, they are not necessarily diagonal in the mass-eigenstate basis. In addition, the ZH^+H^- couplings can differ from the SM ZG^+G^- coupling. This can happen in a general model if H^+ has some admixture of a multiplet larger than a doublet. In the SM, the ZG^+G^- coupling is

$$g_{ZG^+G^-} = -\frac{e}{s_W c_W} \left(\frac{1}{2} - s_W^2 \right). \quad (3.21)$$

4 Charged Higgs corrections to $Z \rightarrow b\bar{b}$

In the SM, the $Zb\bar{b}$ couplings receive a correction from the exchange of the longitudinal components of the W^\pm and Z bosons. The Feynman diagrams for these corrections are shown in fig. 2. We work in the 't Hooft-Feynman gauge, in which the longitudinal components of W^\pm and Z are just the Goldstone bosons G^\pm and G^0 . The diagrams in fig. 2 yield the leading m_t^2 contribution to $\delta g^{L,R}$ in the SM. A detailed review of the calculation of these diagrams is given in ref. [32]. Six additional diagrams, where one or two of the G^\pm lines in fig. 2 is replaced by a

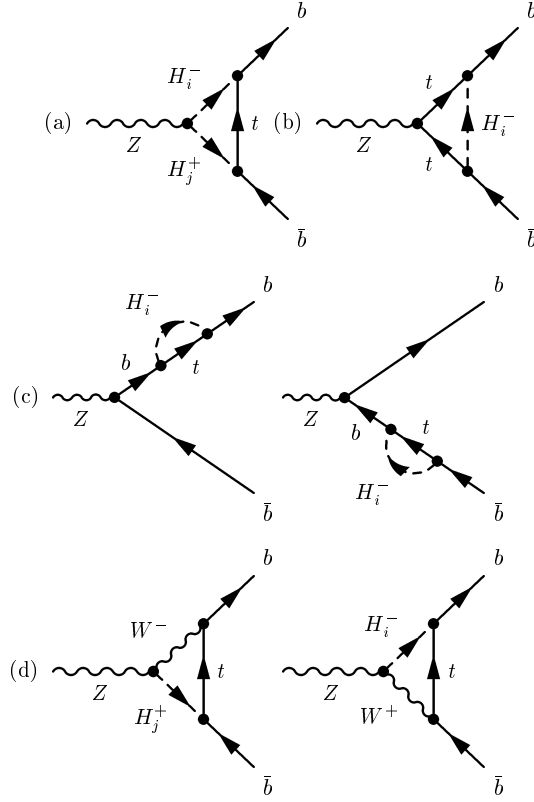


Fig. 3. Feynman diagrams of the electroweak corrections to $Z \rightarrow b\bar{b}$ in a model with an extended Higgs sector.

corresponding W^\pm line, also contribute to $\delta g^{L,R}$. However, the latter contributions are suppressed by a factor of M_Z^2/m_t^2 compared to the diagrams of fig. 2.

In an extended Higgs sector which contains singly charged Higgs states H_i^\pm , the corrections to $\delta g^{L,R}$ arise from the diagrams of fig. 3, where H_i^\pm runs over all the singly charged states in the Higgs sector, including G^\pm .

In calculating the corrections shown in fig. 3 we keep only the leading term in powers of m_t^2/M_Z^2 . In δg^L this leading term is proportional to m_t^2 , where the two powers of m_t come from the left-handed Higgs-quark couplings $g_{H_i^+tb}^L$. In δg^R the right-handed Higgs-quark couplings are proportional to $m_b^2 \tan^2 \beta$, so the leading term in δg^R does not grow with increasing m_t . This approximation has been used in calculating the leading m_t^2 corrections to R_b in the SM in the classic

papers [7,8,9,10], and in calculating the corrections in extended Higgs sectors in refs [16,17,18,19,20].

The two diagrams in fig. 3(d) involving a $ZW^+H_i^-$ vertex can be nonzero in models containing Higgs multiplets larger than doublets. However, their contribution to R_b and A_b is suppressed by a factor of M_Z^2/m_t^2 compared to diagrams 3(a), (b) and (c), and we will neglect them. Diagrams 3(a), (b), and (c) yield

$$\begin{aligned}
\delta g^{L,R}(a) &= \frac{1}{8\pi^2} \sum_{i,j} g_{H_i^+ \bar{t} b}^{L,R} g_{H_j^+ \bar{t} b}^{L,R} g_{ZH_i^+ H_j^-} C_{24}(m_b^2, M_Z^2, m_b^2; m_t^2, M_i^2, M_j^2), \\
\delta g^{L,R}(b) &= -\frac{1}{16\pi^2} \sum_i (g_{H_i^+ \bar{t} b}^{L,R})^2 \left\{ \frac{1}{2} g_{Z\bar{t} t}^{R,L} \right. \\
&\quad \left. + [-2g_{Z\bar{t} t}^{R,L} C_{24} + g_{Z\bar{t} t}^{L,R} m_t^2 C_0] (m_b^2, M_Z^2, m_b^2; M_i^2, m_t^2, m_t^2) \right\}, \\
\delta g^{L,R}(c) &= \frac{1}{16\pi^2} \sum_i \left(g_{H_i^+ \bar{t} b}^{L,R} \right)^2 g_{Z\bar{b} b}^{L,R} B_1(m_b^2; m_t^2, M_i^2). \tag{4.1}
\end{aligned}$$

For the two- and three-point integrals C_{24} , C_0 , and B_1 , we follow the definitions and conventions of ref. [33]. The sums over i and j run over all the singly charged Higgs mass eigenstates H_i^+ as well as the Goldstone boson G^+ . Where no ambiguity is involved, we have given the arguments of groups of tensor integrals that depend on the same variables only once at the end of the group. These expressions for δg^L agree with those of ref. [16].

Collecting the results, and expressing the corrections in terms of the quark Yukawa couplings, we obtain for a Type II model

$$\begin{aligned}
\delta g^L &= -\frac{\lambda_t^2}{16\pi^2} \frac{e}{s_W c_W} \sum_{i,j} \langle H_i^+ | \phi_2^+ \rangle \langle H_j^+ | \phi_2^+ \rangle \\
&\quad \times \left\{ \sum_{k=1}^N \langle H_i^+ | \phi_k^+ \rangle \langle H_j^+ | \phi_k^+ \rangle T_{\phi_k^+}^3 - s_W^2 \delta_{ij} \right\} 2C_{24}(m_t^2, M_i^2, M_j^2) \\
&\quad - \frac{\lambda_t^2}{16\pi^2} \sum_i \langle H_i^+ | \phi_2^+ \rangle^2 \left\{ \frac{1}{2} g_{Z\bar{t} t}^R + [-2g_{Z\bar{t} t}^R C_{24} + g_{Z\bar{t} t}^L m_t^2 C_0] (M_i^2, m_t^2, m_t^2) \right\} \\
&\quad + \frac{\lambda_t^2}{16\pi^2} g_{Z\bar{b} b}^L \sum_i \langle H_i^+ | \phi_2^+ \rangle^2 B_1(m_b^2; m_t^2, M_i^2), \tag{4.2}
\end{aligned}$$

$$\begin{aligned}
\delta g^R &= -\frac{\lambda_b^2}{16\pi^2} \frac{e}{s_W c_W} \sum_{i,j} \langle H_i^+ | \phi_1^+ \rangle \langle H_j^+ | \phi_1^+ \rangle \\
&\quad \times \left\{ \sum_{k=1}^N \langle H_i^+ | \phi_k^+ \rangle \langle H_j^+ | \phi_k^+ \rangle T_{\phi_k^+}^3 - s_W^2 \delta_{ij} \right\} 2C_{24}(m_t^2, M_i^2, M_j^2)
\end{aligned}$$

$$\begin{aligned}
& -\frac{\lambda_b^2}{16\pi^2} \sum_i \langle H_i^+ | \phi_1^+ \rangle^2 \left\{ \frac{1}{2} g_{Zt\bar{t}}^L + \left[-2g_{Zt\bar{t}}^L C_{24} + g_{Zt\bar{t}}^R m_t^2 C_0 \right] (M_i^2, m_t^2, m_t^2) \right\} \\
& + \frac{\lambda_b^2}{16\pi^2} g_{Zb\bar{b}}^R \sum_i \langle H_i^+ | \phi_1^+ \rangle^2 B_1(m_b^2; m_t^2, M_i^2). \tag{4.3}
\end{aligned}$$

For compactness we have dropped the first three arguments of the three–point integrals, (m_b^2, M_Z^2, m_b^2) , because these arguments are the same in all the expressions. The first three arguments of the three–point integrals depend only on the masses of the on–shell external particles.

The corrections for a Type I model are obtained by replacing ϕ_2^+ with ϕ_1^+ in δg^L . We see that δg^L is proportional to λ_t^2 and δg^R is proportional to λ_b^2 . Clearly, δg^R is negligible compared to δg^L , except in a Type II model when λ_b is enhanced for small v_1 . In this situation there is also a significant contribution to $\delta g^{L,R}$ coming from loops involving the neutral Higgs bosons, as described in the next section.

In the Type II 2HDM, δg^R is proportional to $(m_b \tan \beta)^2$, while δg^L is proportional to $(m_t \cot \beta)^2$. At large $\tan \beta$, δg^R is enhanced and δg^L is suppressed; λ_t and λ_b are the same size when $\tan \beta = m_t/m_b \simeq 50$. However, because of their different dependence on the $Zq\bar{q}$ couplings, δg^L and δg^R are the same size when $\tan \beta \simeq 10$.

The formulae in eqs. (4.2)–(4.3) can be simplified. Electromagnetic gauge invariance requires that the terms proportional to s_W^2 (from the $Zq\bar{q}$ and ZH^+H^- couplings) add to zero in the limit $M_Z^2 \rightarrow 0$. This provides a check of our calculations. In our approximation we neglect terms of order M_Z^2/m_t^2 . Using the expansions for the two– and three–point integrals given in ref. [34] and neglecting terms of order M_Z^2/m_t^2 in the three–point integrals, we find that the terms proportional to s_W^2 cancel. The corrections can then be written as

$$\begin{aligned}
\delta g^{L,R} = & \mp \frac{1}{16\pi^2} \frac{e}{s_W c_W} \sum_i \left(g_{H_i^+ t\bar{b}}^{L,R} \right)^2 \frac{1}{2} m_t^2 C_0(M_i^2, m_t^2, m_t^2) \\
& - \frac{1}{16\pi^2} \frac{e}{s_W c_W} \sum_i \left(g_{H_i^+ t\bar{b}}^{L,R} \right)^2 \sum_k \langle H_i^+ | \phi_k^+ \rangle^2 \left(T_{\phi_k^+}^3 - \frac{1}{2} \right) 2C_{24}(m_t^2, M_i^2, M_i^2) \\
& - \frac{1}{16\pi^2} \frac{e}{s_W c_W} \sum_i \sum_{j \neq i} \left(g_{H_i^+ t\bar{b}}^{L,R} \right) \left(g_{H_j^+ t\bar{b}}^{L,R} \right) \sum_k \langle H_i^+ | \phi_k^+ \rangle \langle H_j^+ | \phi_k^+ \rangle T_{\phi_k^+}^3 \\
& \quad \times 2C_{24}(m_t^2, M_i^2, M_j^2). \tag{4.4}
\end{aligned}$$

The third term in eq. (4.4) is the sum of the diagrams 3(a) for two different charged Higgs bosons H_i^+ and H_j^+ in the loop. It is only nonzero when there are nonzero off–diagonal $ZH_i^+H_j^-$ couplings ($i \neq j$). The second term describes the contribution to diagrams 3(a) from diagonal $ZH_i^+H_i^-$ couplings when $T_{\phi_k^+}^3$ is different from 1/2. This term is only nonzero when the Higgs sector contains multiplets larger than doublets. The first term comes from the sum of diagrams 3(b) and (c), plus the

remaining part of diagram 3(a) with $T_{\phi_k^+}^3 = 1/2$. This part of diagram 3(a) is what we would get if we replaced all of the ZH^+H^- couplings with the SM ZG^+G^- coupling. Note that for $m_t \gg M_Z$, $C_0(M_i^2, m_t^2, m_i^2)$ is negative. Therefore the first term of δg^L (δg^R) is always positive (negative) definite, which decreases the prediction for R_b .

From eq. (4.4), one can deduce a number of results. First, if the Higgs sector contains only doublets and singlets, $T_{\phi_k^+}^3 = 1/2$ and there are no off-diagonal ZH^+H^- couplings. Then the second and third terms of eq. (4.4) are zero. We are left with the first term

$$\begin{aligned} \delta g^{L,R} &= \mp \frac{1}{16\pi^2} \frac{e}{2s_W c_W} \sum_i \left(g_{H_i^+ t b}^{L,R} \right)^2 m_t^2 C_0(M_i^2, m_t^2, m_i^2) \\ &= \delta g_{\text{SM}}^{L,R} \pm \frac{1}{16\pi^2} \frac{e}{2s_W c_W} \sum_{i \neq G^+} \left(g_{H_i^+ t b}^{L,R} \right)^2 \left[\frac{R_i}{R_i - 1} - \frac{R_i \log R_i}{(R_i - 1)^2} \right], \end{aligned} \quad (4.5)$$

where $R_i \equiv m_i^2/M_i^2$. The correction in the SM due to G^\pm exchange is denoted by $\delta g_{\text{SM}}^{L,R}$. The non-SM piece of δg^L [δg^R] is positive [negative] definite, both of which decrease R_b . Therefore, in order for it to be possible to increase R_b through charged Higgs boson loops, we must have a Higgs sector that contains multiplets larger than doublets.

Second, if all the H_i^+ are degenerate with G^+ , we can sum over the complete sets of states in the second and third terms of eq. (4.4). These terms cancel and again we are left with

$$\begin{aligned} \delta g^L &= \frac{\lambda_t^2}{16\pi^2} \frac{e}{2s_W c_W} \left[\frac{R}{R-1} - \frac{R \log R}{(R-1)^2} \right], \\ \delta g^R &= -\frac{\lambda_b^2}{16\pi^2} \frac{e}{2s_W c_W} \left[\frac{R}{R-1} - \frac{R \log R}{(R-1)^2} \right], \end{aligned} \quad (4.6)$$

with $R \equiv m_t^2/M_W^2$. This formula includes the SM correction $\delta g_{\text{SM}}^{L,R}$. As above, the non-SM piece of δg^L [δg^R] is positive [negative] definite, both of which decrease R_b .

In a Higgs sector that contains only multiplets for which $\rho = 1$ automatically [eq. (3.7)], the Goldstone boson does not contribute to the second and third terms of eq. (4.4) because there are no off-diagonal $ZG^+H_i^-$ couplings, and the ZG^+G^- coupling is the same as in the SM. Thus in such a model, if all the H_i^+ (excluding G^+) are degenerate with mass M , we can again sum over the complete sets of states in the second and third terms of eq. (4.4). These terms again cancel and we are left with

$$\delta g^L = \delta g_{\text{SM}}^L + \frac{\lambda_t^2}{16\pi^2} \left(1 - \frac{v_2^2}{v_{\text{SM}}^2} \right) \frac{e}{2s_W c_W} \left[\frac{R}{R-1} - \frac{R \log R}{(R-1)^2} \right], \quad (4.7)$$

$$\delta g^R = \delta g_{\text{SM}}^R - \frac{\lambda_b^2}{16\pi^2} \left(1 - \frac{v_1^2}{v_{\text{SM}}^2}\right) \frac{e}{2s_W c_W} \left[\frac{R}{R-1} - \frac{R \log R}{(R-1)^2} \right], \quad (4.8)$$

with $R \equiv m_t^2/M^2$, for a Type II model. The correction in a Type I model is obtained by replacing v_2 with v_1 in eq. (4.7). As above, the non-SM piece of δg^L [δg^R] is positive [negative] definite, both of which decrease R_b .

5 Neutral Higgs corrections to $Z \rightarrow b\bar{b}$

The corrections to $Z \rightarrow b\bar{b}$ from neutral Higgs boson loops, shown in fig. 4, are proportional to λ_b^2 . In a Type I model, $\lambda_b \ll \lambda_t$, so the one-loop radiative corrections mediated by neutral Higgs bosons are negligible compared to charged Higgs mediated corrections (which are proportional to λ_t^2). However, in a Type II model, λ_b increases as v_1 decreases. In the limit of small v_1 , the corrections mediated by neutral Higgs bosons are significant.

In calculating the corrections due to the diagrams in fig. 4, we neglect terms proportional to m_b that are not enhanced by small v_1 . The diagrams of fig. 4(d) are suppressed by a factor of m_b/M_Z compared to diagrams 4(a), (b) and (c), and so we neglect them as well. The contributions to $\delta g^{R,L}$ from diagrams 4(a), (b), and (c) are

$$\begin{aligned} \delta g^{R,L}(a) &= \pm \frac{1}{4\pi^2} \sum_{H_i^0, A_j^0} g_{ZH_i^0 A_j^0} g_{H_i^0 b\bar{b}}^V g_{A_j^0 b\bar{b}}^A C_{24}(m_b^2, M_i^2, M_j^2) \\ &= \mp \frac{\lambda_b^2}{8\pi^2} \frac{e}{s_W c_W} \sum_{H_i^0, A_j^0} \langle H_i^0 | \phi_1^{0,r} \rangle \langle A_j^0 | \phi_1^{0,i} \rangle \sum_{k=1}^N \langle H_i^0 | \phi_k^{0,r} \rangle \langle A_j^0 | \phi_k^{0,i} \rangle T_{\phi_k^0}^3 C_{24}(m_b^2, M_i^2, M_j^2), \\ \delta g^{R,L}(b) &= -\frac{1}{16\pi^2} g_{Zb\bar{b}}^{L,R} \left[\sum_{H_i^0} (g_{H_i^0 b\bar{b}}^V)^2 \left\{ \frac{1}{2} - [2C_{24} + M_Z^2(C_{22} - C_{23})] (M_i^2, m_b^2, m_b^2) \right\} \right. \\ &\quad \left. - \sum_{A_j^0} (g_{A_j^0 b\bar{b}}^A)^2 \left\{ \frac{1}{2} - [2C_{24} + M_Z^2(C_{22} - C_{23})] (M_j^2, m_b^2, m_b^2) \right\} \right] \\ &= -\frac{\lambda_b^2}{32\pi^2} g_{Zb\bar{b}}^{L,R} \left[\sum_{H_i^0} \langle H_i^0 | \phi_1^{0,r} \rangle^2 \left\{ \frac{1}{2} - [2C_{24} + M_Z^2(C_{22} - C_{23})] (M_i^2, m_b^2, m_b^2) \right\} \right. \\ &\quad \left. + \sum_{A_j^0} \langle A_j^0 | \phi_1^{0,i} \rangle^2 \left\{ \frac{1}{2} - [2C_{24} + M_Z^2(C_{22} - C_{23})] (M_j^2, m_b^2, m_b^2) \right\} \right], \end{aligned}$$

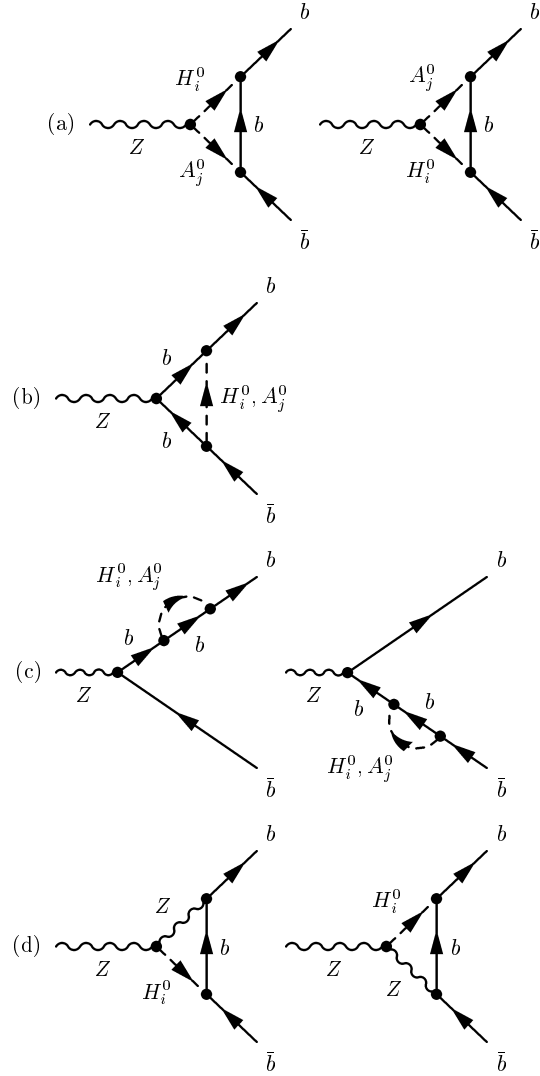


Fig. 4. Feynman diagrams for the corrections to $Z \rightarrow b\bar{b}$ involving neutral Higgs bosons in the loop.

$$\begin{aligned}
\delta g^{R,L}(c) &= \frac{1}{16\pi^2} g_{Zb\bar{b}}^{R,L} \left[\sum_{H_i^0} (g_{H_i^0 b\bar{b}}^V)^2 B_1(m_b^2; m_b^2, M_i^2) - \sum_{A_j^0} (g_{A_j^0 b\bar{b}}^A)^2 B_1(m_b^2; m_b^2, M_j^2) \right] \\
&= \frac{\lambda_b^2}{32\pi^2} g_{Zb\bar{b}}^{R,L} \left[\sum_{H_i^0} \langle H_i^0 | \phi_1^{0,r} \rangle^2 B_1(m_b^2; m_b^2, M_i^2) + \sum_{A_j^0} \langle A_j^0 | \phi_1^{0,i} \rangle^2 B_1(m_b^2; m_b^2, M_j^2) \right]. \quad (5.1)
\end{aligned}$$

For compactness of notation, we again drop the first three arguments, (m_b^2, M_Z^2, m_b^2) , of the three-point integrals. Note that $g_{ZH_i^0 A_j^0}$ and $g_{A_j^0 b\bar{b}}^A$ are imaginary, while $g_{H_i^0 b\bar{b}}^V$ is real. In the sums over scalar states, H_i^0 runs over all CP-even neutral Higgs bosons, and A_j^0 runs over all CP-odd neutral Higgs bosons (including G^0). However, the corrections involving G^0 can be neglected because the G^0 coupling to $b\bar{b}$ is not enhanced by large λ_b . In particular, $g_{G^0 b\bar{b}}^A = -m_b/v_{\text{SM}}$, independent of the value of v_1 .

As in section 4, we can use electromagnetic gauge invariance to check our calculations. Electromagnetic gauge invariance requires that terms proportional to s_W^2 sum to zero in the limit $M_Z \rightarrow 0$. Note that $\delta g^{R,L}(a)$ is independent of s_W^2 , whereas in the limit $M_Z \rightarrow 0$, $\delta g^{R,L}(b) + \delta g^{R,L}(c) = 0$, independent of the Higgs masses. The terms proportional to s_W^2 indeed vanish in this limit.

Finally, we briefly examine the special case in which all the H_i^0 are degenerate with mass M_H , and all the A_j^0 (excluding G^0) are degenerate with mass M_A . In this case, we can sum over complete sets of states and eq. (5.1) simplifies to

$$\begin{aligned}
\delta g^{R,L}(a) &= \pm \frac{\lambda_b^2}{16\pi^2} \left(\frac{e}{s_W c_W} \right) C_{24}(m_b^2, M_H^2, M_A^2), \\
\delta g^{R,L}(b) &= -\frac{\lambda_b^2}{32\pi^2} g_{Zb\bar{b}}^{L,R} \left\{ 1 - \left[2C_{24} + M_Z^2(C_{22} - C_{23}) \right] (M_H^2, m_b^2, m_b^2) \right. \\
&\quad \left. - \left[2C_{24} + M_Z^2(C_{22} - C_{23}) \right] (M_A^2, m_b^2, m_b^2) \right\}, \\
\delta g^{R,L}(c) &= \frac{\lambda_b^2}{32\pi^2} g_{Zb\bar{b}}^{R,L} \left[B_1(m_b^2; m_b^2, M_H^2) + B_1(m_b^2; m_b^2, M_A^2) \right]. \quad (5.2)
\end{aligned}$$

6 Corrections to $Z \rightarrow b\bar{b}$ in specific extended Higgs models

In this section we calculate the radiative corrections to $Z \rightarrow b\bar{b}$ in a variety of extended Higgs models, and ascertain the constraints on the parameter space of each model due to the experimental data. We find that the corrections to R_b are large enough that the measured value of R_b can be used to constrain the parameter space of specific models. However, the corrections to A_b are small compared to the uncertainty in the measurement of A_b , and thus cannot be used to further constrain the models.

6.1 Models with Higgs doublets and singlets

6.1.1 Charged Higgs boson contributions

In a model containing only Higgs doublets and singlets, the radiative corrections due to the charged Higgs bosons are described by eq. (4.5). These corrections have definite signs; in particular, $\delta g^L > 0$ and $\delta g^R < 0$. Both of these give $\Delta R_b < 0$, in worse agreement with experiment than the SM. The corrections due to neutral Higgs boson exchange will also contribute when λ_b is enhanced. They must be taken into account as well in this regime when deriving constraints from the R_b measurement.

Two Higgs doublet model The 2HDM contains a single charged Higgs boson,

$$H^+ = -\sin\beta\phi_1^+ + \cos\beta\phi_2^+. \quad (6.1)$$

Its contribution to $\delta g^{L,R}$ is found from eq. (4.5) with only one H^+ in the sum. For the Type II 2HDM,

$$\delta g^L = \frac{1}{32\pi^2} \left(\frac{gm_t}{\sqrt{2}M_W} \cot\beta \right)^2 \frac{e}{s_W c_W} \left[\frac{R}{R-1} - \frac{R \log R}{(R-1)^2} \right], \quad (6.2)$$

$$\delta g^R = -\frac{1}{32\pi^2} \left(\frac{gm_b}{\sqrt{2}M_W} \tan\beta \right)^2 \frac{e}{s_W c_W} \left[\frac{R}{R-1} - \frac{R \log R}{(R-1)^2} \right], \quad (6.3)$$

where $R \equiv m_t^2/M_{H^+}^2$. This correction is in addition to the correction due to Goldstone boson exchange, which is the same as in the SM. This agrees with the results of refs. [16,17,18,19,20]. In the Type II model, δg^L is significant at small $\tan\beta$ and is suppressed at large $\tan\beta$, while δg^R is negligible at small $\tan\beta$ but is significant at large $\tan\beta$.

In a Type I model the result is the same except that $\cot^2\beta$ is replaced with $\tan^2\beta$ in δg^L . In this case, δg^R is negligible compared to δg^L at any value of $\tan\beta$. Both δg^L and δg^R grow with increasing $\tan\beta$.

For small $\tan\beta$, the neutral Higgs couplings to b quarks are small, and contributions to $Z \rightarrow b\bar{b}$ due to neutral Higgs boson exchange can be neglected. In this regime the corrections due to charged Higgs boson exchange can be used to constrain the 2HDM. In fig. 5 we plot the constraints from R_b on M_{H^+} as a function of $\tan\beta$, for a Type II 2HDM. We also show the constraints on the charged Higgs mass from the process $b \rightarrow s\gamma$ [35,36] and the charged Higgs boson search at LEP [37]. The constraint on the charged Higgs mass from the Tevatron D0 experiment [38] is significantly weaker than the constraint from $b \rightarrow s\gamma$, and are not shown in fig. 5. R_b provides the strongest constraint on M_{H^+} for $\tan\beta < 1.5$. For larger $\tan\beta$, the constraint from $b \rightarrow s\gamma$ is stronger.

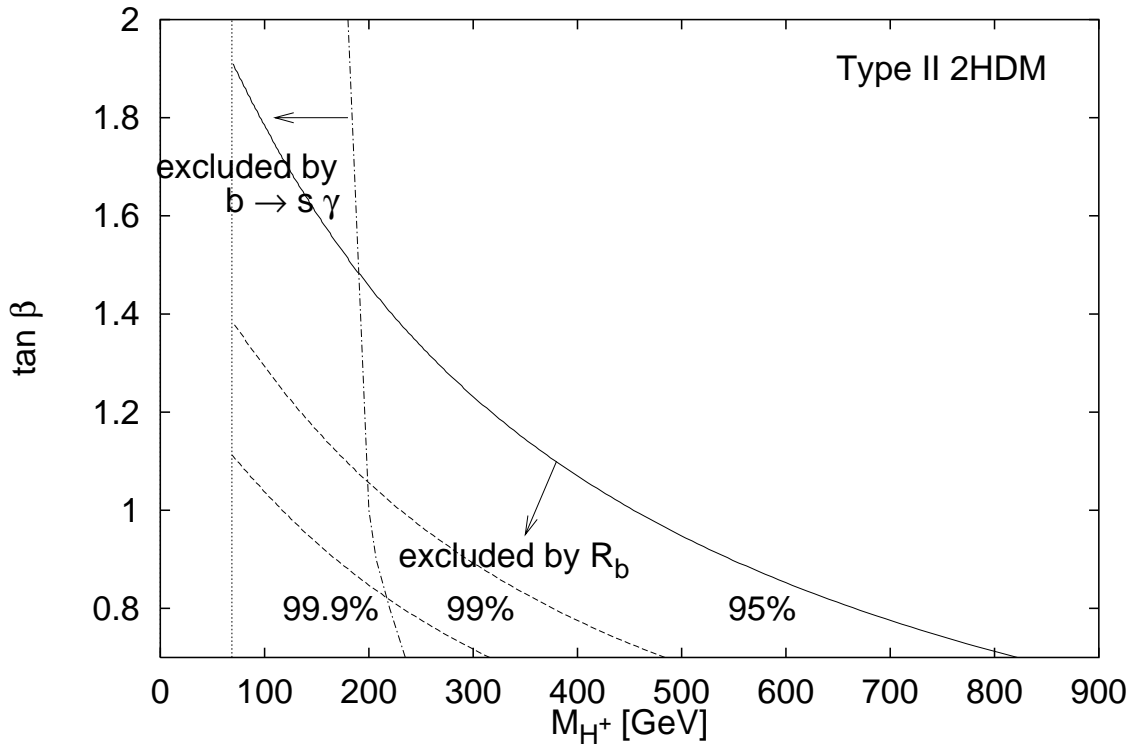


Fig. 5. Constraints from R_b on the charged Higgs mass and $\tan \beta$ in the Type II 2HDM. The area below the solid line is excluded at 95% confidence level. Also shown are the 99% and 99.9% confidence levels (dashed lines). We also show the 95% confidence level lower bound on M_{H^+} from the $b \rightarrow s\gamma$ branching ratio [35,36] (dot-dashed). The vertical dotted line is the direct search bound on the charged Higgs mass, $M_{H^+} > 77.3$ GeV [37].

For large $\tan\beta$, neutral Higgs boson exchange contributes to $Z \rightarrow b\bar{b}$ in addition to charged Higgs boson exchange. The neutral Higgs boson contributions are discussed in section 6.1.2.

In the case of a Type I 2HDM, the bound on M_{H^+} from R_b is the same as in fig. 5, but with $\cot\beta$ replacing $\tan\beta$ on the vertical axis. In this class of models there is no constraint at present on the charged Higgs boson mass from $b \rightarrow s\gamma$.

Multiple-doublet models and models with singlets We now consider the effects of charged Higgs boson exchange in a model containing multiple Higgs doublets, denoted Φ_k , with $Y = 1$. We can add to this model any number of Higgs singlets with zero hypercharge. These contain only neutral degrees of freedom, and so they have no effect on the charged Higgs sector.

In a Type I model of this type, we let Φ_1 couple to both up- and down-type quarks, and none of the other doublets couple to quarks. In a Type II model, we let Φ_1 couple only to down-type quarks, and Φ_2 couple to up-type quarks. Then the Yukawa couplings are defined in the same way as in the 2HDM, in eqs. (3.10)–(3.11).

In a Type II model, the contributions to $Z \rightarrow b\bar{b}$ from charged Higgs boson exchange are

$$\delta g^L = \frac{1}{32\pi^2} \frac{e}{s_W c_W} \left(\frac{gm_t}{\sqrt{2}M_W} \frac{v_{\text{SM}}}{v_2} \right)^2 \sum_{i \neq G^+} \langle H_i^+ | \phi_2^+ \rangle^2 \left[\frac{R_i}{R_i - 1} - \frac{R_i \log R_i}{(R_i - 1)^2} \right], \quad (6.4)$$

$$\delta g^R = -\frac{1}{32\pi^2} \frac{e}{s_W c_W} \left(\frac{gm_b}{\sqrt{2}M_W} \frac{v_{\text{SM}}}{v_1} \right)^2 \sum_{i \neq G^+} \langle H_i^+ | \phi_1^+ \rangle^2 \left[\frac{R_i}{R_i - 1} - \frac{R_i \log R_i}{(R_i - 1)^2} \right] \quad (6.5)$$

where $R_i \equiv m_t^2/M_{H_i^+}^2$. This contribution is in addition to the contribution due to charged Goldstone boson exchange, which is the same as in the SM. In a Type I model, the contribution is the same except that v_2 is replaced with v_1 and ϕ_2^+ is replaced with ϕ_1^+ in the formula for δg^L .

These corrections to $\delta g^{L,R}$ from charged Higgs boson exchange have the same dependence on the charged Higgs masses as the corrections in the 2HDM. The contribution from each H_i^+ is weighted by the overlap of each H_i^+ with the electroweak eigenstate that couples to the quarks involved.

Note that the Yukawa couplings depend on the ratios v_{SM}/v_2 and v_{SM}/v_1 . This is the same dependence as in the 2HDM. Recall that in the 2HDM, v_1 and v_2 were constrained by the W mass to satisfy the relation, $v_1^2 + v_2^2 = v_{\text{SM}}^2$. Thus in the 2HDM, v_1 and v_2 cannot both be small at the same time. However, in a model with more than two doublets, the W mass constraint involves the vevs of all the doublets (labeled by k), giving $\sum_k v_k^2 = v_{\text{SM}}^2$. In this model, both v_1 and v_2 can be small at the same time, leading to significant contributions to both δg^L and δg^R .

The corrections to $Z \rightarrow b\bar{b}$ in this model can be understood by examining their behavior in certain limits. First, let us examine the limit in which all but one of the H_i^+ are very heavy. The contributions of the heavy H_i^+ to $\delta g^{L,R}$ go to zero as the masses go to infinity. The remaining contribution to $\delta g^{L,R}$ is due to the single light charged Higgs boson, and it is of the same form as in the 2HDM. Comparing with eqs. (6.2)–(6.3), we see that in δg^L , $\tan\beta$ is replaced by $v_2/[v_{\text{SM}}\langle H_i^+|\phi_2^+\rangle]$, and in δg^R , $\tan\beta$ is replaced by $[v_{\text{SM}}\langle H_i^+|\phi_1^+\rangle]/v_1$. The charged Higgs sector can be constrained by R_b when there are no significant contributions to $Z \rightarrow b\bar{b}$ coming from neutral Higgs boson exchange. This is ensured when v_1 is not too small. In this regime, δg^L can be significant, while δg^R is negligible. The constraint from R_b on the mass of the remaining light charged Higgs boson is the same as in fig. 5, with $\tan\beta$ replaced by $v_2/[v_{\text{SM}}\langle H_i^+|\phi_2^+\rangle]$.

If v_2 and $\langle H_i^+|\phi_2^+\rangle$ are held constant while the masses of the heavy charged Higgs bosons are reduced, the bound shown in fig. 5 becomes stronger. This happens because the heavy charged Higgs bosons begin to contribute to δg^L , forcing the contribution of the light charged Higgs boson to be smaller in order to be consistent with the measured value of R_b . This is done by raising the mass of the light charged Higgs boson.

Finally, if all the charged Higgs bosons are degenerate, with a common mass M_H , then we can sum over a complete set of states and the corrections in a Type II model simplify to the following:

$$\delta g^L = \frac{1}{32\pi^2} \frac{e}{s_W c_W} \left(\frac{gm_t}{\sqrt{2}M_W} \right)^2 \frac{v_{\text{SM}}^2 - v_2^2}{v_2^2} \left[\frac{R}{R-1} - \frac{R \log R}{(R-1)^2} \right], \quad (6.6)$$

$$\delta g^R = \frac{1}{32\pi^2} \frac{e}{s_W c_W} \left(\frac{gm_b}{\sqrt{2}M_W} \right)^2 \frac{v_{\text{SM}}^2 - v_1^2}{v_1^2} \left[\frac{R}{R-1} - \frac{R \log R}{(R-1)^2} \right], \quad (6.7)$$

where $R \equiv m_t^2/M_H^2$. These corrections are in addition to the corrections due to charged Goldstone boson exchange in the SM. In a Type I model, v_2 is replaced by v_1 in δg^L .

These corrections are the same as the corrections in the 2HDM, with $\tan\beta$ replaced by $v_2/(v_{\text{SM}}^2 - v_2^2)^{1/2}$ in δg^L , and $\tan\beta$ replaced by $(v_{\text{SM}}^2 - v_1^2)^{1/2}/v_1$ in δg^R . As before, the charged Higgs sector can be constrained by R_b when there are no significant contributions to $Z \rightarrow b\bar{b}$ coming from neutral Higgs boson exchange. This is ensured when v_1 is not too small. In this regime, the constraint from R_b on the common charged Higgs mass M_H is the same as in fig. 5, with $\tan\beta$ replaced by $v_2/(v_{\text{SM}}^2 - v_2^2)^{1/2}$.

6.1.2 Neutral Higgs boson contributions

As we showed in section 5, the radiative corrections to the process $Z \rightarrow b\bar{b}$ due to neutral Higgs boson exchange are proportional to λ_b^2 . They are negligible compared to the contributions from charged Higgs boson exchange which are proportional to λ_t^2 , except when λ_b is enhanced relative to λ_t . This happens in a Type II model when $v_1 \ll v_2$. In what follows we consider only Type II models. When λ_b is enhanced, the corrections to δg^R due to charged Higgs boson exchange will also contribute. These must be taken into account when deriving constraints on Higgs sector parameters from the R_b measurement.

Two Higgs doublet model The 2HDM contains three neutral Higgs bosons,

$$\begin{aligned} A^0 &= -\sin\beta\phi_1^{0,i} + \cos\beta\phi_2^{0,i}, \\ h^0 &= -\sin\alpha\phi_1^{0,r} + \cos\alpha\phi_2^{0,r}, \\ H^0 &= \cos\alpha\phi_1^{0,r} + \sin\alpha\phi_2^{0,r}. \end{aligned} \tag{6.8}$$

The corrections due to neutral Higgs boson exchange in the 2HDM depend on the masses of the three neutral Higgs bosons, the mixing angle α , and $\tan\beta \equiv v_2/v_1$. The Higgs couplings are easily found from these parameters using the formulae of section 3 (see, *e.g.*, ref. [11]). Inserting these couplings into eq. (5.1) for the corrections from neutral Higgs boson exchange

$$\begin{aligned} \delta g^{R,L}(a) &= \pm \frac{1}{16\pi^2} \frac{e}{s_W c_W} \left(\frac{gm_b}{\sqrt{2}M_W} \right)^2 \tan^2\beta \\ &\quad \times \left[\frac{s_\alpha}{s_\beta} \cos(\beta - \alpha) C_{24}(m_b^2, M_{h^0}^2, M_{A^0}^2) + \frac{c_\alpha}{s_\beta} \sin(\beta - \alpha) C_{24}(m_b^2, M_{H^0}^2, M_{A^0}^2) \right], \\ \delta g^{R,L}(b) &= -\frac{1}{32\pi^2} g_{Zb\bar{b}}^{L,R} \left(\frac{gm_b}{\sqrt{2}M_W} \right)^2 \tan^2\beta \\ &\quad \times \left[\left(\frac{s_\alpha}{s_\beta} \right)^2 \left\{ \frac{1}{2} - [2C_{24} + M_Z^2(C_{22} - C_{23})] (M_{h^0}^2, m_b^2, m_b^2) \right\} \right. \\ &\quad \left. + \left(\frac{c_\alpha}{s_\beta} \right)^2 \left\{ \frac{1}{2} - [2C_{24} + M_Z^2(C_{22} - C_{23})] (M_{H^0}^2, m_b^2, m_b^2) \right\} \right. \\ &\quad \left. + \frac{1}{2} - [2C_{24} + M_Z^2(C_{22} - C_{23})] (M_{A^0}^2, m_b^2, m_b^2) \right], \\ \delta g^{R,L}(c) &= \frac{1}{32\pi^2} g_{Zb\bar{b}}^{R,L} \left(\frac{gm_b}{\sqrt{2}M_W} \right)^2 \tan^2\beta \end{aligned}$$

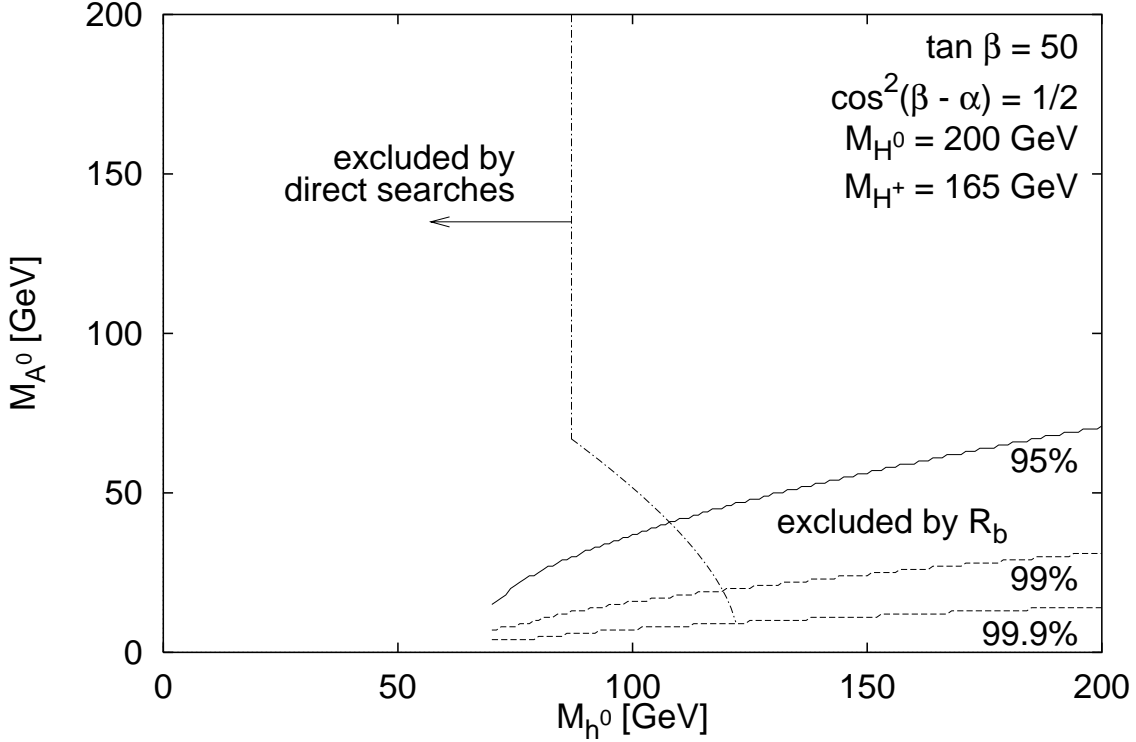


Fig. 6. R_b in the 2HDM with $\tan\beta = 50$, $\cos^2(\beta - \alpha) = 1/2$, $M_{H^0} = 200$ GeV and $M_{H^+} = 165$ GeV. $\Delta R_b < 0$ for all allowed masses, so this model is in worse agreement with experiment than the SM. The solid line is the 95% confidence level lower bound on M_{A^0} from R_b . Also shown are the 99% and 99.9% confidence level contours (dashed lines). The dot-dashed line is the lower bound on M_{h^0} from direct searches (see appendix B).

$$\times \left[\left(\frac{s_\alpha}{s_\beta} \right)^2 B_1(m_b^2; m_b^2, M_{h^0}^2) + \left(\frac{c_\alpha}{s_\beta} \right)^2 B_1(m_b^2; m_b^2, M_{H^0}^2) + B_1(m_b^2; m_b^2, M_{A^0}^2) \right] \quad (6.9)$$

where $s_\alpha \equiv \sin\alpha$, $c_\alpha \equiv \cos\alpha$, $s_\beta \equiv \sin\beta$, and $c_\beta \equiv \cos\beta$.

The contribution of these corrections to R_b can be either positive or negative, depending on the neutral Higgs masses and the mixing angle α . We plot the corrections for various sets of parameters.

In fig. 6, we plot the constraints on the neutral Higgs sector from R_b . The parameters in this plot are $\tan\beta = 50$, $\cos^2(\beta - \alpha) = 1/2$, and $M_{H^0} = 200$ GeV. With $\cos^2(\beta - \alpha) = 1/2$, the Zh^0A^0 and ZH^0A^0 couplings are equal, and h^0 , H^0 , and A^0 all contribute to the corrections. The contribution of the charged Higgs boson (which depends on M_{H^+}) to R_b must also be considered. Note that for large $\tan\beta$, the charged Higgs boson contributions to δg^L are negligible, whereas contributions to δg^R are negative which reduces R_b . In fig. 6, we have taken

$M_{H^+} = 165$ GeV, which is the lower bound on the charged Higgs mass in the general 2HDM based on constraints from the observed rate for $b \rightarrow s\gamma$ [35,36]. We can also consider a second case where $M_{H^+} \gg M_Z$. In this limit, the contribution of H^+ to R_b vanishes, and we need only consider the effects of the neutral Higgs sector.⁴ However, given a fixed value of M_{H^0} , one cannot arbitrarily increase M_{H^+} without violating the constraints due to the ρ -parameter. In appendix A, the shift in the ρ -parameter due to one-loop radiative corrections mediated by the non-minimal Higgs sector of the 2HDM is given by eq. (A.1). As an example, consider the case of $\cos^2(\beta - \alpha) = 1/2$ and $M_{h^0}, M_{A^0} \leq M_{H^0} = 200$ GeV as in fig. 6. If we take $\Delta\rho \lesssim 3 \times 10^{-3}$, we find that the charged Higgs boson must be lighter than about 270 GeV. For $M_{H^+} = 270$ GeV, the contour lines in fig. 6 change by an insignificant amount, so there is no need to show a separate graph.

Since the corrections to R_b from both the charged and neutral Higgs bosons are proportional to $\tan^2\beta$, we can vary $\tan\beta$ within the large $\tan\beta$ regime and ΔR_b will still be negative. In particular, the region ruled out by R_b gets larger as $\tan\beta$ increases. In fig. 6, the range of masses of h^0 and A^0 in which $\Delta R_b > 0$ is already excluded by direct searches. For all remaining allowed h^0 and A^0 masses, $\Delta R_b < 0$, in worse agreement with experiment than the SM. The corresponding corrections to A_b are negligible ($|\Delta A_b| < 0.003$) compared to the experimental uncertainty in the A_b measurement.

In fig. 7, we exhibit the constraints on the neutral Higgs sector from R_b for $\cos(\beta - \alpha) = 1$, with all other parameters the same as in fig. 6. For $\cos(\beta - \alpha) = 1$, the ZH^0A^0 coupling is zero and the $H^0b\bar{b}$ coupling is not enhanced over the SM $H^0b\bar{b}$ coupling, so the contribution of H^0 to the corrections is negligible. The region where $\Delta R_b > 0$ (due to the positive contribution of the neutral Higgs bosons to R_b which overcomes the negative contribution from H^+ exchange) lies below the (roughly) semi-circular dashed contour. However, this region of parameter space is already ruled out by the direct search limits from LEP (see appendix B). Note that the corrections to R_b are negative for large splittings between M_{h^0} and M_{A^0} . Thus areas of low M_{h^0} and high M_{A^0} , and of low M_{A^0} and high M_{h^0} , are ruled out by the R_b measurement. Again, the corresponding corrections to A_b are negligible ($|\Delta A_b| < 0.004$) compared to the experimental uncertainty in the A_b measurement.

Both the charged and neutral Higgs boson corrections at large $\tan\beta$ are proportional to $\tan^2\beta$. Hence, varying $\tan\beta$ will not change the combinations of M_{h^0} and M_{A^0} for which $\Delta R_b = 0$. It follows that the line where R_b is equal to its SM value stays the same as we vary $\tan\beta$, as long as we remain in the large $\tan\beta$ regime. Since the corrections grow with $\tan\beta$, the regions ruled out by R_b in fig. 7 get larger as $\tan\beta$ increases.

As previously noted, the corrections from charged Higgs boson exchange give

⁴Since $\Delta R_b < 0$ from virtual H^+ exchange, in the case of $M_{H^+} \rightarrow \infty$, the R_b exclusion contours in fig. 6 would move downward (*i.e.*, less parameter space would be excluded).

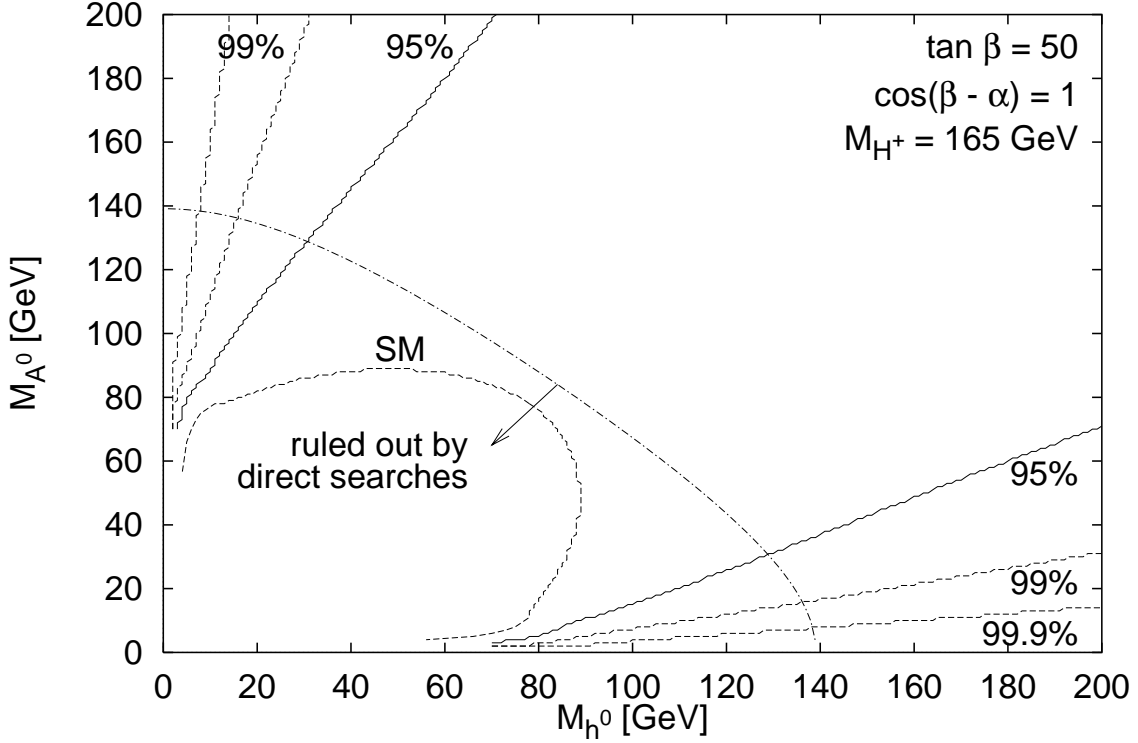


Fig. 7. R_b in the Type II 2HDM with $\tan \beta = 50$, $\cos(\beta - \alpha) = 1$, and $M_{H^+} = 165$ GeV. The solid lines are the 95% confidence level lower bounds on M_{A^0} and M_{h^0} from R_b . The 99% and 99.9% confidence level bounds from R_b are also indicated by the appropriately labeled dashed lines. The (roughly) semi-circular dashed line labeled “SM” is where the predicted value of R_b is the same as in the SM. The region below this line, in which $\Delta R_b > 0$, is entirely excluded by direct searches (see appendix B). The latter region corresponds to the area below the dot-dashed line in the direction indicated by the arrow.

a negative contribution to R_b . If the charged Higgs mass is increased, its negative contribution is reduced, and hence the excluded regions of fig. 6 shrink. In particular, the semi-circular contour where $\Delta R_b = 0$ moves outward, and eventually crosses the dot-dashed line (which indicates the boundary of the region excluded by direct searches). That is, for large enough H^+ mass, there exists an unexcluded region of the M_{h^0} vs. M_{A^0} plane for which $R_b > 0$, resulting in a slightly better fit to the measured value of R_b . However, as noted above, the charged Higgs mass cannot be taken too large without violating the ρ -parameter constraint. If this constraint is also imposed, then even with M_{H^+} taken at its maximally allowed value (with the parameters as given in fig. 6), the viable region of parameter space where $R_b > 0$ is quite small. Moreover, this region is on the verge of being ruled out by the direct Higgs searches at LEP.

Finally, we can consider the case of $\cos(\beta - \alpha) = 0$ by interchanging the roles of h^0 and H^0 in fig. 7; the results for R_b and A_b will remain the same. For $\cos(\beta - \alpha) = 0$, the couplings of h^0 are equal to their SM values, so the SM Higgs search limit applies. That is, the experimental lower limit of M_{h^0} is equivalent to the SM Higgs mass bound from LEP, $M_{h^0} > 95.2$ GeV [37]. H^0 is, by definition, the heavier CP-even neutral Higgs boson, so $M_{H^0} > M_{h^0} > 95.2$ GeV. The mass of H^0 is also constrained by the LEP search for $H^0 A^0$ production. When $\cos(\beta - \alpha) = 0$, the $Z h^0 A^0$ coupling is zero and the $h^0 b \bar{b}$ coupling is not enhanced over the SM coupling. Hence, h^0 does not contribute significantly to the corrections and we will neglect it.

The constraints on the Higgs parameters from R_b for $\cos(\beta - \alpha) = 0$ are shown in fig. 8. To ensure that the ρ -parameter is satisfied, we have set $M_{H^+} = M_{A^0}$ for $M_{A^0} > 165$ GeV. For $M_{A^0} < 165$ GeV, we have taken $M_{H^+} = 165$ GeV, to be consistent with the constraint from $b \rightarrow s \gamma$ [35,36]. The R_b measurement rules out areas of parameter space where the mass splitting between H^0 and A^0 is large. For example, if the H^0 (A^0) mass is 1000 GeV, then A^0 (H^0) must be heavier than about 300 GeV.

Two Higgs doublet model in the decoupling limit In the decoupling limit of the 2HDM, h^0 remains light and its couplings to the SM particles approach those of the SM Higgs boson, while all the other Higgs bosons become heavy and nearly degenerate in mass. In particular, in the decoupling limit [39]: (i) $M_{h^0} \sim \mathcal{O}(M_Z)$; (ii) $M_{H^0} \simeq M_{A^0} \simeq M_{H^+} \gg M_Z$; (iii) $|M_{H^0}^2 - M_{A^0}^2| \sim |M_{H^+}^2 - M_{A^0}^2| \sim \mathcal{O}(M_Z^2)$; and (iv) $\cos(\beta - \alpha) \sim \mathcal{O}(M_Z^2/M_{A^0}^2)$. We can expand the corrections to $Z \rightarrow b \bar{b}$ from neutral Higgs boson exchange in the 2HDM in this limit. Expanding the three-point integrals in the limit of $M_{A^0} \gg M_Z$ (see, *e.g.*, ref. [34]), we obtain to leading order in $M_Z^2/M_{A^0}^2$:

$$\delta g^L \simeq \frac{1}{16\pi^2} \left(\frac{e}{s_W c_W} \right) \left(\frac{g m_b}{\sqrt{2} M_W} \right)^2 \tan^2 \beta \frac{M_Z^2}{M_{A^0}^2} \left\{ -\frac{1}{36} + \frac{1}{9} s_W^2 \left[\frac{1}{3} + \log \left(-\frac{M_{A^0}^2}{M_Z^2} \right) \right] \right\},$$

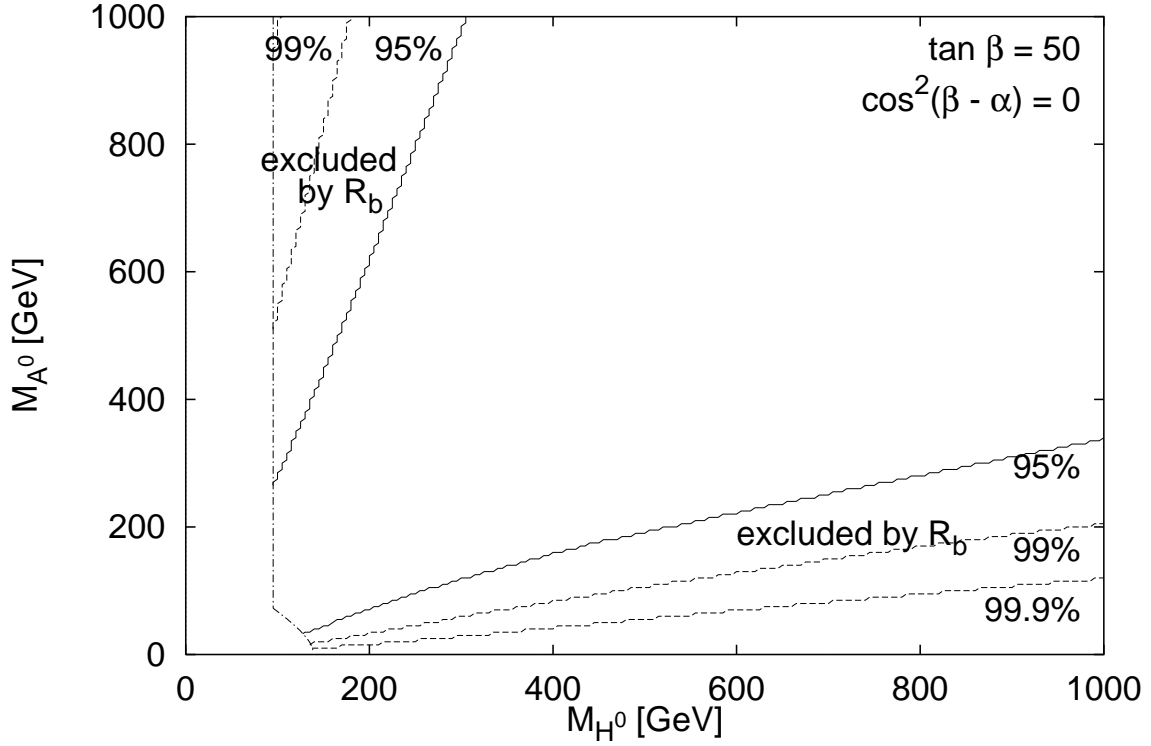


Fig. 8. R_b in the 2HDM with $\tan \beta = 50$ and $\cos(\beta - \alpha) = 0$. For $M_{A^0} > 165$ GeV, we take $M_{H^+} = M_{A^0}$, while for $M_{A^0} < 165$ GeV, we take $M_{H^+} = 165$ GeV. The solid lines are the 95% confidence level lower bounds on M_{A^0} and M_{H^0} from R_b . The labeled dashed lines are the 99% and 99.9% confidence level bounds from R_b . The dot-dashed line is the bound from direct searches (see appendix B).

$$\delta g^R \simeq \frac{1}{16\pi^2} \left(\frac{e}{s_W c_W} \right) \left(\frac{g m_b}{\sqrt{2} M_W} \right)^2 \tan^2 \beta \times \frac{M_Z^2}{M_{A^0}^2} \left\{ -\frac{1}{36} - \frac{1}{6} \left[\log \left(-\frac{M_{A^0}^2}{M_Z^2} \right) \right] + \frac{1}{9} s_W^2 \left[\frac{1}{3} + \log \left(-\frac{M_{A^0}^2}{M_Z^2} \right) \right] \right\}. \quad (6.10)$$

As an example, for $\tan \beta = 50$ and $M_{A^0} = 200$ GeV, the above corrections give $\Delta R_b = -3.7 \times 10^{-4}$, which is only half the size of the experimental error of the R_b measurement. The corrections vanish in the limit of large M_{A^0} as expected from decoupling. This limit is approached in fig. 8 when M_{H^0} and M_{A^0} are both large (compared to M_Z) and similar in size.

Multiple-doublet models We now consider neutral Higgs boson exchange in a model containing multiple Higgs doublets, denoted Φ_k , with hypercharge $Y = 1$.

In a Type I model of this type, we let Φ_1 couple to both up- and down-type quarks, and none of the other doublets couple to quarks. In a Type II model, we let Φ_1 couple only to down-type quarks, and Φ_2 couple to up-type quarks. Then the Yukawa couplings are defined in the same way as in the 2HDM, in eqs. (3.10)–(3.11). As always, the contributions to $Z \rightarrow b\bar{b}$ from neutral Higgs boson exchange are only significant in a Type II model, when λ_b is enhanced by small v_1 . We will only consider Type II multi-doublet models with small v_1 .

The contributions from neutral Higgs boson exchange in the multi-doublet model are more complicated than in the 2HDM, simply because there are more neutral Higgs states. Only the states which have a nonzero overlap with Φ_1 can couple to b quarks, so only these states contribute. The corrections depend on the overlap of each neutral state with Φ_1 and the mass of each state. As in the 2HDM, the region of parameter space in which the correction to R_b is positive is almost entirely ruled out by direct searches.

Multiple-doublet models with Higgs singlets We can also consider adding a number of Higgs singlets, with hypercharge zero, to the multi-doublet model. The singlets do not couple to Z or to quarks. Their vevs are also unconstrained by the W mass. In general, the singlets will mix with the neutral components of the doublets to form mass eigenstates. The couplings of the physical states to $b\bar{b}$ still depend only on v_1 , which fixes λ_b , and on the overlap of each state with Φ_1 . The couplings of physical states to Z are no longer the same as in a model containing only doublets. Instead, they are equal to the Z coupling for doublet states weighted by the overlap of each state with doublets. Explicitly,

$$g_{ZH_i^0 A_j^0} = \frac{-ie}{2s_W c_W} \sum_k \langle H_i^0 | \phi_k^{0,r} \rangle \langle A_j^0 | \phi_k^{0,i} \rangle, \quad (6.11)$$

where k runs only over the Higgs doublets.

In order to understand the effects of singlets on the corrections to $Z \rightarrow b\bar{b}$, let us imagine replacing each Higgs singlet with the neutral component of a doublet, with the appropriate CP quantum number, while holding the masses and mixings of the physical states fixed. Then, the couplings of each state to $b\bar{b}$ remain the same. However, the couplings of the states to Z are now equal to,

$$g_{ZH_i^0 A_j^0} = \frac{-ie}{2s_W c_W}, \quad (6.12)$$

which is the coupling in a model containing only Higgs doublets. Comparing this to eq. (6.11), we see that $\delta g^{R,L}(a)$ in the model with singlets must be smaller in magnitude than in the model in which the singlets are replaced by doublets.

Degenerate neutral Higgs bosons in a general extended Higgs sector

The corrections to $Z \rightarrow b\bar{b}$ due to neutral Higgs boson exchange in a general model are quite complicated. They depend on the couplings and masses of all the neutral Higgs bosons in the model. However, the corrections can be simplified if some of the neutral Higgs bosons are degenerate in mass.

Consider a general extended Higgs sector, which can contain Higgs singlets, doublets, and larger multiplets. We require that the model be Type II, and that λ_b be enhanced relative to λ_t . A Type II model must contain at least two Higgs doublets, Φ_1 and Φ_2 , to couple to down- and up-type quarks, respectively. Only the neutral Higgs bosons with large couplings to $b\bar{b}$ give significant contributions to the corrections. In what follows we will only consider these. States without enhanced $b\bar{b}$ couplings, such as G^0 , do not contribute significantly. We will ignore them, and therefore it does not matter what their masses are.

If all the CP-even neutral Higgs bosons are degenerate with mass M_H , and all the CP-odd neutral Higgs bosons are degenerate with mass M_A , then we can take the two- and three-point integrals outside of the sums in eq. (5.1). Then we can sum the couplings over complete sets of states. Using the couplings in a general model from eqs. (3.13), (3.14) and (3.17), we find

$$\sum_{H_i^0, A_j^0} g_{ZH_i^0 A_j^0} g_{H_i^0 b\bar{b}}^V g_{A_j^0 b\bar{b}}^A = \frac{e}{2s_W c_W} \left(\frac{gm_b}{\sqrt{2}M_W} \right)^2 \left(\frac{v_{\text{SM}}}{v_1} \right)^2, \quad (6.13)$$

$$\sum_{H_i^0} (g_{H_i^0 b\bar{b}}^V)^2 = - \sum_{A_j^0} (g_{A_j^0 b\bar{b}}^A)^2 = \left(\frac{gm_b}{\sqrt{2}M_W} \right)^2 \left(\frac{v_{\text{SM}}}{v_1} \right)^2. \quad (6.14)$$

These sums over the couplings are related to certain couplings in the 2HDM, as follows. On the left-hand side are the couplings in the general model with degenerate neutral Higgs bosons, and on the right-hand side are the couplings in the

2HDM with $\cos(\beta - \alpha) = 1$. That is,

$$\sum_{H_i^0, A_j^0} g_{ZH_i^0 A_j^0} g_{H_i^0 b\bar{b}}^V g_{A_j^0 b\bar{b}}^A = g_{Zh^0 A^0} g_{h^0 b\bar{b}}^V g_{A^0 b\bar{b}}^A, \quad (6.15)$$

$$\sum_{H_i^0} (g_{H_i^0 b\bar{b}}^V)^2 = (g_{h^0 b\bar{b}}^V)^2, \quad (6.16)$$

$$\sum_{A_j^0} (g_{A_j^0 b\bar{b}}^A)^2 = (g_{A^0 b\bar{b}}^A)^2. \quad (6.17)$$

Therefore, when all the CP–even neutral Higgs bosons are degenerate with mass M_H , and all the CP–odd neutral Higgs bosons are degenerate with mass M_A , the contributions to $Z \rightarrow b\bar{b}$ are the same as the contributions from the 2HDM with $M_{h^0} = M_H$, $M_{A^0} = M_A$, and $\cos(\beta - \alpha) = 1$. The parameter corresponding to $\tan\beta$ in the extended model is

$$\frac{v_{\text{SM}}^2 - v_1^2}{v_1^2} = \tan^2 \beta. \quad (6.18)$$

Similarly, the corrections can be simplified if only the CP–even states, or only the CP–odd states, are degenerate. If the CP–even states are degenerate, we can sum over the H_i^0 couplings. We then get the same result as if the CP–even neutral Higgs sector consisted of a single state H^0 , which consists entirely of $\phi_1^{0,r}$. Recall that $\phi_1^{0,r}$ is the CP–even neutral component of the doublet which couples to down–type quarks. If, instead, the CP–odd states are degenerate, we can sum over the A_j^0 couplings. We get the same result as if the CP–odd neutral Higgs sector consisted of a single state A^0 , which consists entirely of $\phi_1^{0,i}$ (up to the small mixing of $\phi_1^{0,i}$ with G^0 , which is negligible in the small v_1 regime).

6.2 Models with Higgs multiplets larger than doublets

We next consider Higgs sectors that contain one or more multiplets larger than doublets. Two types of models that use different approaches to satisfy $\rho \simeq 1$ are examined. We first consider models in which the vevs of the multiplets larger than doublets are fine-tuned to be very small, so that their contribution to the ρ parameter is negligible. Second, we consider models that preserve $\text{SU}(2)_c$ symmetry (in the Higgs sector), ensuring that $\rho = 1$ at tree level.

6.2.1 Models with one Higgs doublet and one triplet

The minimal extension of the Higgs sector that includes multiplets larger than doublets consists of the complex $Y = 1$ doublet of the SM, denoted by Φ , plus a triplet Higgs field. The vev of the triplet field must be fine-tuned very small in

order to be consistent with the measured value of the ρ parameter, $\rho \simeq 1$. The triplet field can either be a real triplet with $Y = 0$, or a complex triplet with $Y = 2$. Here we investigate both possibilities.

These two models contain only one Higgs doublet, which couples to both up- and down-type quarks, so they are necessarily Type I models. Thus $\lambda_b \ll \lambda_t$, and the only non-negligible contributions to $Z \rightarrow b\bar{b}$ come from the contributions to δg^L from charged Higgs boson exchange.

We first consider the “ $Y = 0$ model” with one doublet and one real triplet field with $Y = 0$. The triplet field is $\xi = (\xi^+, \xi^0, \xi^-)$. We define the doublet and triplet vevs by $\langle \phi^0 \rangle = v_\phi/\sqrt{2}$ and $\langle \xi^0 \rangle = v_\xi$. The vevs are constrained by the W mass to satisfy

$$v_{\text{SM}}^2 = v_\phi^2 + 4v_\xi^2. \quad (6.19)$$

It is convenient to parameterize the ratio of the vevs by

$$\tan \theta_0 = \frac{v_\phi}{2v_\xi}. \quad (6.20)$$

In this model, the tree-level ρ parameter is

$$\rho = \frac{v_\phi^2 + 4v_\xi^2}{v_\phi^2} = 1 + \frac{4v_\xi^2}{v_\phi^2} \equiv 1 + \Delta\rho. \quad (6.21)$$

In terms of $\tan \theta_0$, we find

$$\Delta\rho = \frac{1}{\tan^2 \theta_0}. \quad (6.22)$$

We see that in order to have $\rho \simeq 1$, the triplet vev must be very small, giving large $\tan \theta_0$. The charged states mix to form the charged Goldstone boson and a single charged physical state

$$\begin{aligned} G^+ &= \sin \theta_0 \phi^+ + \cos \theta_0 \xi^+, \\ H^+ &= \cos \theta_0 \phi^+ - \sin \theta_0 \xi^+. \end{aligned} \quad (6.23)$$

We next consider the “ $Y = 2$ model” with one doublet and one complex triplet field with $Y = 2$. The triplet field is $\chi = (\chi^{++}, \chi^+, \chi^0)$. We define the vev of this triplet field by $\langle \chi^0 \rangle = v_\chi/\sqrt{2}$. The vevs are constrained by the W mass to satisfy

$$v_{\text{SM}}^2 = v_\phi^2 + 2v_\chi^2. \quad (6.24)$$

It is convenient to parameterize the ratio of the doublet and triplet vevs by

$$\tan \theta_2 = \frac{v_\phi}{\sqrt{2}v_\chi}. \quad (6.25)$$

In this model, the tree-level ρ parameter is

$$\rho = \frac{v_\phi^2 + 2v_\chi^2}{v_\phi^2 + 4v_\chi^2} = 1 - \frac{2v_\chi^2}{v_\phi^2 + 4v_\chi^2} \equiv 1 + \Delta\rho. \quad (6.26)$$

In terms of $\tan\theta_2$, we find

$$\Delta\rho = \frac{-1}{\tan^2\theta_2 + 2}. \quad (6.27)$$

We see that in order to have $\rho \simeq 1$, the triplet vev must be very small, giving large $\tan\theta_2$. The charged states mix to form the charged Goldstone boson and a single charged physical state

$$\begin{aligned} G^+ &= \sin\theta_2 \phi^+ + \cos\theta_2 \xi^+, \\ H^+ &= \cos\theta_2 \phi^+ - \sin\theta_2 \xi^+. \end{aligned} \quad (6.28)$$

The Higgs couplings to quarks and the Z boson can be parameterized as follows. We let θ denote θ_0 in the $Y = 0$ model and θ_2 in the $Y = 2$ model. We also define a factor ϵ such that $\epsilon = +1$ in the $Y = 0$ model and $\epsilon = -1$ in the $Y = 2$ model. The charged Higgs couplings to quarks are

$$g_{G^+ \bar{b} b}^L = \frac{gm_t}{\sqrt{2}M_W}, \quad (6.29)$$

$$g_{H^+ \bar{b} b}^L = \frac{gm_t}{\sqrt{2}M_W} \cot\theta. \quad (6.30)$$

The $ZH_i^+H_j^-$ couplings are

$$g_{ZG^+G^-} = -\frac{e}{s_W c_W} \left(\frac{1}{2} - s_W^2 + \frac{\epsilon}{2} \cos^2\theta \right), \quad (6.31)$$

$$g_{ZG^+H^-} = \frac{e}{s_W c_W} \frac{\epsilon}{2} \sin\theta \cos\theta, \quad (6.32)$$

$$g_{ZH^+H^-} = -\frac{e}{s_W c_W} \left(\frac{1}{2} - s_W^2 + \frac{\epsilon}{2} \sin^2\theta \right). \quad (6.33)$$

Contributions to $Z \rightarrow b\bar{b}$ In both the $Y = 0$ and the $Y = 2$ models, there is an off-diagonal ZG^+H^- coupling, and the diagonal ZH^+H^- and ZG^+G^- couplings differ from their values in models containing only Higgs doublets and singlets. These couplings contribute to the second and third terms of δg^L in eq. (4.4).

In addition to the SM contribution to δg_{SM}^L from G^+ exchange, the charged Higgs contribution to δg^L is given by

$$\begin{aligned} \delta g^L &= \frac{1}{32\pi^2} \left(\frac{gm_t}{\sqrt{2}M_W} \right)^2 \frac{e}{s_W c_W} \cos^2\theta \left\{ \frac{1}{\sin^2\theta} \left[\frac{R}{R-1} - \frac{R \log R}{(R-1)^2} \right] \right. \\ &\quad \left. - 2\epsilon \left[C_{24}(m_t^2, M_W^2, M_W^2) + C_{24}(m_t^2, M_{H^+}^2, M_{H^+}^2) - 2C_{24}(m_t^2, M_W^2, M_{H^+}^2) \right] \right\} \quad (6.34) \end{aligned}$$

where $R \equiv m_t^2/M_{H^+}^2$.

Note that δg^L is proportional to $\cos^2 \theta$, which goes to zero in the large $\tan \theta$ limit. This is due to the fact that in the limit of small triplet vev in either of these models, the overlap of H^+ with the doublet is proportional to $\cos \theta$. As a result, in the large $\tan \theta$ limit, H^+ is almost entirely triplet and so its couplings to quarks are very small. Also in the large $\tan \theta$ limit, the off-diagonal ZG^+H^- coupling goes to zero, and the ZG^+G^- coupling approaches its SM value.

Constraints from the ρ parameter We must also take into account the constraint on $\tan \theta$ from the ρ parameter in each of the models. Since $\Delta\rho$ depends differently on $\tan \theta_0$ than on $\tan \theta_2$, the constraint on $\tan \theta$ will be different in the $Y = 0$ model than in the $Y = 2$ model.

The experimental constraints on $\Delta\rho$ are taken from ref. [5]. Writing the tree-level value of the ρ -parameter as $\rho = 1 + \Delta\rho_{\text{new}}$, the 2σ level limits are:

$$-1.7 \times 10^{-3} < \Delta\rho_{\text{new}} < 2.7 \times 10^{-3}. \quad (6.35)$$

We now use $\Delta\rho_{\text{new}}$ to constrain $\tan \theta_0$ and $\tan \theta_2$. We ignore the radiative corrections from the non-minimal Higgs sector. In the $Y = 0$ model, $\Delta\rho_{\text{new}} > 0$, while in the $Y = 2$ model, $\Delta\rho_{\text{new}} < 0$. The resulting 2σ limits on $\tan \theta_0$ and $\tan \theta_2$ are:

$$\tan \theta_0 > 19, \quad \tan \theta_2 > 24. \quad (6.36)$$

Results The contribution to δg^L in both the $Y = 0$ model and the $Y = 2$ model is proportional to $\cos^2 \theta$ [eq. (6.34)]. When the constraints on $\tan \theta$ from the ρ parameter are imposed, the corrections to R_b and A_b are very small. Even allowing for the largest possible values of θ_0 and θ_2 , we find that over the relevant Higgs parameter space (with M_{H^+} varying between 10 and 1000 GeV), $|\Delta R_b| < 7 \times 10^{-6}$ and $|\Delta A_b| < 3 \times 10^{-6}$. These corrections are tiny compared to the experimental error on the R_b and A_b measurements [eqs. (2.8) and (2.9)].

In general, the contribution to δg^L vanishes in the large $\tan \theta$ limit in any model in which the charged Goldstone boson is made up almost entirely of the doublet that couples to quarks. As a result, the overlap of the other charged Higgs states with the doublet is very small, so the other charged Higgs states couple very weakly to quarks. This occurs in any model that contains only one scalar doublet, plus any number of singlets and multiplets larger than doublets, as long as the vevs of the multiplets larger than doublets are forced to be small.

The contributions of multiplets larger than doublets to $Z \rightarrow b\bar{b}$ can be large only if the larger multiplets mix significantly with doublets, so that the resulting Higgs states have non-negligible couplings to quarks. This can happen in two ways. First, if the model contains more than one doublet, then each singly-charged scalar field of the doublets that couples to quarks will contain physical scalar components that

can mix with charged scalar states from higher multiplets. The resulting physical charged scalar mass eigenstates can thus possess a non-negligible couplings to quarks. A model of this type is discussed in section 6.2.2. Second, if the multiplets larger than doublets have sizeable vevs, then the charged Goldstone boson must contain some admixture of the larger multiplets, leaving part of the doublet free to mix into the physical charged Higgs states. However, in order for the multiplets larger than doublets to have sizeable vevs without violating the constraint from the ρ parameter, the model must preserve $SU(2)_c$ symmetry. Models of this type are discussed in section 6.2.3.

6.2.2 Models with two doublets and one triplet

We next consider a Higgs sector consisting of two doublets and one triplet. As in section 6.2.1, the triplet can be real with $Y = 0$ or complex with $Y = 2$. The couplings for these models are given in ref. [24]. With two doublets, we can construct either a Type I model or a Type II model. In this section we consider a Type II model, but we also note the changes in the formulae that must be made to recover a Type I model.

We will consider both the corrections due to charged Higgs boson exchange and the corrections due to neutral Higgs boson exchange. The corrections from neutral Higgs boson exchange can be significant in a Type II model with large $\tan\beta$. We define $\tan\beta$ in this model exactly as in the 2HDM, $\tan\beta = v_2/v_1$, where the vevs of the doublets are $\langle\phi_1^0\rangle = v_1/\sqrt{2}$ and $\langle\phi_2^0\rangle = v_2/\sqrt{2}$.

Charged Higgs boson contributions We first consider the corrections due to charged Higgs boson exchange in the “ $Y = 0$ model” consisting of two doublets and one real triplet field with $Y = 0$. The triplet field is $\xi = (\xi^+, \xi^0, \xi^-)$. We define the triplet vev by $\langle\xi^0\rangle = v_\xi$. In the $Y = 0$ model we parameterize the vevs by

$$\tan\theta_0 = \frac{(v_1^2 + v_2^2)^{1/2}}{2v_\xi}, \quad (6.37)$$

in analogy to section 6.2.1.

The charged Higgs states are defined as follows. The Goldstone boson is

$$G^+ = \sin\theta_0(\cos\beta\phi_1^+ + \sin\beta\phi_2^+) + \cos\theta_0\xi^+. \quad (6.38)$$

In addition we define two orthogonal states

$$\begin{aligned} H_1^{+'} &= \cos\theta_0(\cos\beta\phi_1^+ + \sin\beta\phi_2^+) - \sin\theta_0\xi^+, \\ H_2^{+'} &= -\sin\beta\phi_1^+ + \cos\beta\phi_2^+, \end{aligned} \quad (6.39)$$

which will mix by an angle δ to form the mass eigenstates. Before mixing them, however, let us take the limit of large $\tan\theta_0$ in order to satisfy the experimental constraint on the ρ -parameter. We make the approximation that $\sin\theta_0 \approx 1$ and $\cos\theta_0 \approx 0$ (the general case of arbitrary $\tan\theta_0$ is considered in ref. [24]). Then the positively charged scalar states are

$$\begin{aligned} G^+ &\simeq \cos\beta\phi_1^+ + \sin\beta\phi_2^+, \\ H_1^{+'} &\simeq -\xi^+, \\ H_2^{+'} &= -\sin\beta\phi_1^+ + \cos\beta\phi_2^+, \end{aligned} \quad (6.40)$$

These states mix by an angle δ to form the mass eigenstates:

$$\begin{aligned} H_1^+ &\simeq \sin\delta(-\sin\beta\phi_1^+ + \cos\beta\phi_2^+) - \cos\delta\xi^+, \\ H_2^+ &\simeq \cos\delta(-\sin\beta\phi_1^+ + \cos\beta\phi_2^+) + \sin\delta\xi^+. \end{aligned} \quad (6.41)$$

We next consider the corrections due to charged Higgs boson exchange in the “ $Y = 2$ model” consisting of two doublets and one complex triplet field with $Y = 2$. The triplet field is $\chi = (\chi^{++}, \chi^+, \chi^0)$. We define the triplet vev by $\langle\chi^0\rangle = v_\chi/\sqrt{2}$. In the $Y = 2$ model we parameterize the vevs by

$$\tan\theta_2 = \frac{(v_1^2 + v_2^2)^{1/2}}{\sqrt{2}v_\chi}, \quad (6.42)$$

again in analogy to section 6.2.1.

The charged Higgs states in the $Y = 2$ model are parameterized in the same way as the states in the $Y = 0$ model. The Goldstone boson is

$$G^+ = \sin\theta_2(\cos\beta\phi_1^+ + \sin\beta\phi_2^+) + \cos\theta_2\chi^+. \quad (6.43)$$

In addition we define two orthogonal states:

$$\begin{aligned} H_1^{+'} &= \cos\theta_2(\cos\beta\phi_1^+ + \sin\beta\phi_2^+) - \sin\theta_2\chi^+, \\ H_2^{+'} &= -\sin\beta\phi_1^+ + \cos\beta\phi_2^+, \end{aligned} \quad (6.44)$$

which will mix by an angle δ to form the mass eigenstates. Before mixing them, we shall take the limit of large $\tan\theta_2$ in order to satisfy the experimental constraint on the ρ -parameter. We make the approximation $\sin\theta_2 \approx 1$ and $\cos\theta_2 \approx 0$ (the general case of arbitrary $\tan\theta_2$ is considered in ref. [24]). Then the positively charged scalar states are

$$\begin{aligned} G^+ &\simeq \cos\beta\phi_1^+ + \sin\beta\phi_2^+, \\ H_1^{+'} &\simeq -\chi^+, \\ H_2^{+'} &= -\sin\beta\phi_1^+ + \cos\beta\phi_2^+. \end{aligned} \quad (6.45)$$

These states mix by an angle δ to form the mass eigenstates:

$$\begin{aligned} H_1^+ &\simeq \sin \delta (-\sin \beta \phi_1^+ + \cos \beta \phi_2^+) - \cos \delta \chi^+, \\ H_2^+ &\simeq \cos \delta (-\sin \beta \phi_1^+ + \cos \beta \phi_2^+) + \sin \delta \chi^+. \end{aligned} \quad (6.46)$$

The states and couplings for arbitrary $\tan \theta_2$ are given in ref. [24].

We now calculate the corrections to $Z \rightarrow b\bar{b}$ from charged Higgs boson exchange in the Type II $Y = 0$ and $Y = 2$ models. As in section 6.2.1, we introduce the parameter $\epsilon = +1$ in the $Y = 0$ model, and $\epsilon = -1$ in the $Y = 2$ model. In addition to the SM correction due to charged Goldstone boson exchange, the charged Higgs contributions to δg^L are given by

$$\begin{aligned} \delta g^L &\simeq \frac{1}{32\pi^2} \frac{e}{s_W c_W} \left(\frac{gm_t}{\sqrt{2}M_W} \right)^2 \cot^2 \beta \\ &\times \left\{ \sin^2 \delta \left[\frac{R_1}{R_1 - 1} - \frac{R_1 \log R_1}{(R_1 - 1)^2} \right] + \cos^2 \delta \left[\frac{R_2}{R_2 - 1} - \frac{R_2 \log R_2}{(R_2 - 1)^2} \right] \right\} \\ &- \frac{\epsilon}{16\pi^2} \frac{e}{s_W c_W} \left(\frac{gm_t}{\sqrt{2}M_W} \right)^2 \cot^2 \beta \sin^2 \delta \cos^2 \delta \\ &\times \left[C_{24}(m_t^2, M_{H_1^+}^2, M_{H_1^+}^2) + C_{24}(m_t^2, M_{H_2^+}^2, M_{H_2^+}^2) - 2C_{24}(m_t^2, M_{H_1^+}^2, M_{H_2^+}^2) \right] \end{aligned} \quad (6.47)$$

where $R_i \equiv m_t^2/M_{H_i^+}^2$. In the Type I models, δg^L is the same as above with $\cot^2 \beta$ replaced by $\tan^2 \beta$.

The first term of eq. (6.47) is the same as the correction in a three Higgs doublet model (3HDM), given in eq. (6.4). It is positive, which gives a negative contribution to R_b , taking it farther from the measured value. The second term comes from the effects of the triplet. This second term is proportional to $\sin^2 \delta \cos^2 \delta$, so it is only significant for δ near $\pi/4$, which corresponds to maximal mixing between the charged doublet and triplet states in H_1^+ and H_2^+ . The second term is zero if H_1^+ and H_2^+ have the same mass.

The sign of the second term depends on the hypercharge of the Higgs triplet. In the $Y = 0$ model, the second term is negative. However, the second term is smaller in magnitude than the first term, so the overall contribution to δg^L is positive in the $Y = 0$ model. In fig. 9, we plot the constraints on $M_{H_1^+}$ and $M_{H_2^+}$ from the R_b measurement in the $Y = 0$ model, for maximal doublet–triplet mixing ($\delta = \pi/4$) and $\tan \beta = 1$. In order for the $Y = 0$ model with maximal doublet–triplet mixing to be consistent with the R_b measurement, one or both of the charged Higgs bosons must be very heavy.

In the $Y = 2$ model, the second term of eq. (6.47) is positive, resulting in a positive δg^L which is larger than in the $Y = 0$ model. As a result, a larger area of

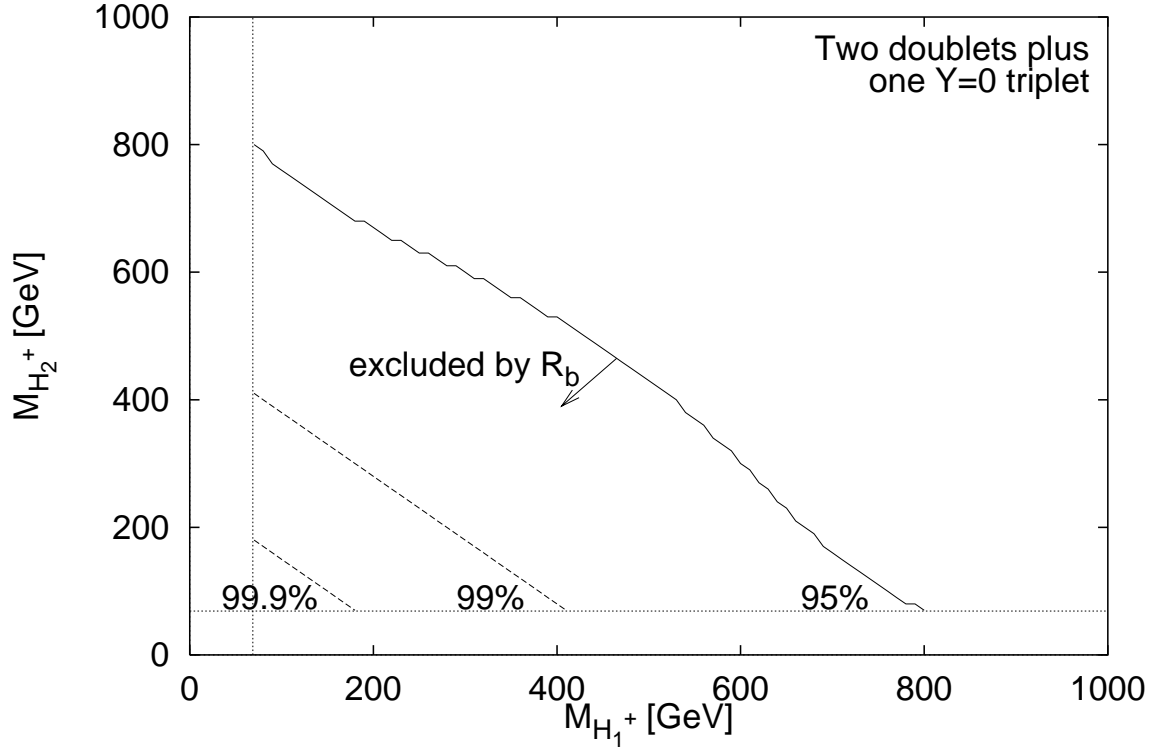


Fig. 9. Constraints from R_b on the masses of the two charged Higgs states H_1^+ and H_2^+ in the model with two doublets and one real $Y = 0$ triplet, with $\tan \beta = 1$ and $\delta = \pi/4$. The area below the solid line is excluded at 95% confidence level. Also shown are the 99% and 99.9% confidence levels (dashed). The dotted lines correspond to the LEP lower limit for the H^+ mass, $M_{H^+} > 77.3$ GeV [37].

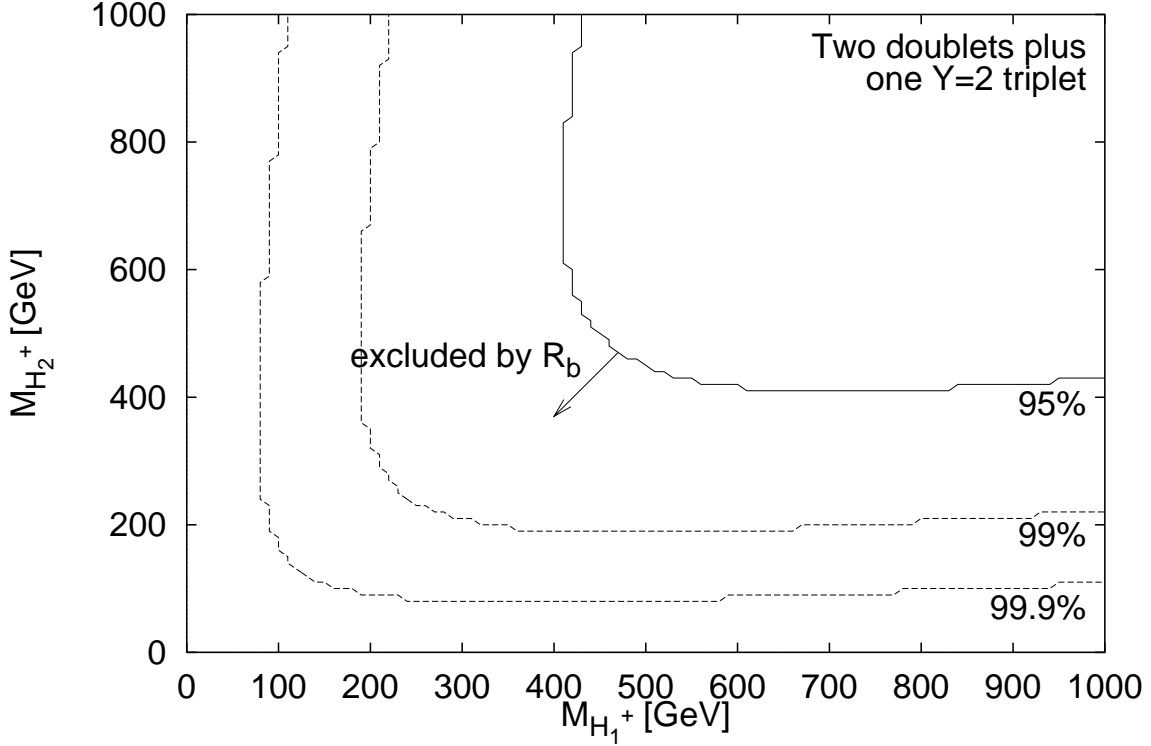


Fig. 10. Constraints from R_b on the masses of the two charged Higgs states H_1^+ and H_2^+ in the model with two doublets and one complex $Y = 2$ triplet, with $\tan\beta = 1$ and $\delta = \pi/4$. The area below the solid line is excluded at 95% confidence level. For these values of $\tan\beta$ and δ , H^+ masses below 410 GeV are ruled out. Also shown are the 99% and 99.9% confidence levels (dashed).

parameter space is excluded by the R_b measurement in the $Y = 2$ model than in the $Y = 0$ model. In fig. 10, we plot the constraints on $M_{H_1^+}$ and $M_{H_2^+}$ from the R_b measurement on the $Y = 2$ model, for maximal doublet–triplet mixing ($\delta = \pi/4$) and $\tan\beta = 1$. From the R_b constraint with these parameters, we find that both of the charged Higgs bosons must be heavier than 410 GeV. If δ is varied or $\tan\beta$ is increased, this bound becomes lower. Note that we do not plot a direct search bound on the H^+ mass. In this model, the LEP bound on the charged Higgs mass does not apply, as explained in appendix B.

For completeness, we also write the contributions to δg^R , which are only significant at large $\tan\beta$. For both the Type I and Type II models

$$\delta g^R \simeq -\frac{1}{32\pi^2} \frac{e}{s_W c_W} \left(\frac{gm_b}{\sqrt{2}M_W} \right)^2 \tan^2\beta$$

$$\begin{aligned}
& \times \left\{ \sin^2 \delta \left[\frac{R_1}{R_1 - 1} - \frac{R_1 \log R_1}{(R_1 - 1)^2} \right] + \cos^2 \delta \left[\frac{R_2}{R_2 - 1} - \frac{R_2 \log R_2}{(R_2 - 1)^2} \right] \right\} \\
& - \frac{\epsilon}{16\pi^2} \frac{e}{s_W c_W} \left(\frac{gm_b}{\sqrt{2}M_W} \right)^2 \tan^2 \beta \sin^2 \delta \cos^2 \delta \\
& \times \left[C_{24}(m_t^2, M_{H_1^+}^2, M_{H_1^+}^2) + C_{24}(m_t^2, M_{H_2^+}^2, M_{H_2^+}^2) - 2C_{24}(m_t^2, M_{H_1^+}^2, M_{H_2^+}^2) \right] \quad (6.48)
\end{aligned}$$

where $\epsilon = +1$ in the $Y = 0$ model and $\epsilon = -1$ in the $Y = 2$ model. The first term of eq.(6.48) is the same as the correction in a 3HDM. The second term comes from the effects of the triplet.

Neutral Higgs boson contributions Consider the contributions to $Z \rightarrow b\bar{b}$ from neutral Higgs boson exchange in these models. The corrections can only be significant in the Type II models when $\tan \beta$ is large. For this reason, we disregard the Type I models here.

In the $Y = 0$ model, there is no $Z\xi^0 A^0$ coupling [24]. As a result, ξ^0 has the same couplings as a Higgs singlet. Thus, the corrections from neutral Higgs boson exchange have the same form as in a model containing two doublets and a real singlet with $Y = 0$. Models of this type were discussed in section 6.1.2.

In the $Y = 2$ model, there are nonzero $Z\chi^{0,r}\chi^{0,i}$ couplings [24]. The neutral Higgs states can be written in the large $\tan \theta_2$ limit as

$$H_1^0 = \cos \gamma (\cos \alpha \phi_1^{0,r} + \sin \alpha \phi_2^{0,r}) + \sin \gamma \chi^{0,r}, \quad (6.49)$$

$$H_2^0 = -\sin \gamma (\cos \alpha \phi_1^{0,r} + \sin \alpha \phi_2^{0,r}) + \cos \gamma \chi^{0,r}, \quad (6.50)$$

$$H_3^0 = -\sin \alpha \phi_1^{0,r} + \cos \alpha \phi_2^{0,r}, \quad (6.51)$$

$$G^0 \simeq \cos \beta \phi_1^{0,i} + \sin \beta \phi_2^{0,i}, \quad (6.52)$$

$$A_1^0 \simeq -\sin \omega \sin \beta \phi_1^{0,i} + \sin \omega \cos \beta \phi_2^{0,i} - \cos \omega \chi^{0,i}, \quad (6.53)$$

$$A_2^0 \simeq -\cos \omega \sin \beta \phi_1^{0,i} + \cos \omega \cos \beta \phi_2^{0,i} + \sin \omega \chi^{0,i}, \quad (6.54)$$

where, for simplicity, only H_1^0 and H_2^0 contain triplet admixtures. We find that the contributions of the neutral Higgs bosons in this model can be split into two pieces. The first piece is the same as the contribution in a 3HDM, in which the neutral Higgs states are given as above but with the triplet states $\chi^{0,r}$ and $\chi^{0,i}$ replaced by the neutral states of the third doublet. This piece is denoted by $\delta g_{3\text{HDM}}^{R,L}$. The second piece contains the additional contribution due to the effects of the isospin and hypercharge of the triplet, and is denoted $\delta g_{\text{triplet}}^{R,L}$. That is,

$$\delta g^{R,L} = \delta g_{3\text{HDM}}^{R,L} + \delta g_{\text{triplet}}^{R,L}. \quad (6.55)$$

Explicit formulae can be found in ref. [24]. One finds that $\delta g_{\text{triplet}}^{R,L}$ is only significant near maximal doublet–triplet mixing in both the CP–odd and CP–even

sectors, which occurs when ω and γ are both near $\pm\pi/4$. In addition, $\delta g_{\text{triplet}}^{R,L}$ is zero if $M_{H_1^0} = M_{H_2^0}$ or $M_{A_1^0} = M_{A_2^0}$. Its sign depends on the mixing angles and the Higgs masses. For all the neutral Higgs bosons lighter than about 200 GeV and maximal doublet–triplet mixing, the contribution to R_b from $\delta g_{\text{triplet}}^{R,L}$ is smaller than the contribution to R_b from $\delta g_{3\text{HDM}}^{R,L}$ over most of the parameter space. The contribution to R_b from $\delta g_{3\text{HDM}}^{R,L}$ is of the same order of magnitude as the contribution to R_b from the neutral sector of the 2HDM.

6.2.3 Georgi–Machacek model with $SU(2)_c$ symmetry

In order to obtain $\rho = 1$ at tree level the electroweak symmetry breaking must preserve a “custodial” $SU(2)$ symmetry, called $SU(2)_c$, that ensures equal masses are given to the W^\pm and W^3 . We refer to models with this property as generalized Georgi–Machacek (G–M) models, after the extended model of this type with Higgs triplets first introduced in ref. [40].

The triplet G–M model contains a complex $Y = 1$ doublet Φ , a real $Y = 0$ triplet ξ , and a complex $Y = 2$ triplet χ . The Higgs fields take the form

$$\Phi = \begin{pmatrix} \phi^{0*} & \phi^+ \\ -\phi^{+*} & \phi^0 \end{pmatrix} \quad (6.56)$$

$$\chi = \begin{pmatrix} \chi^{0*} & \xi^+ & \chi^{++} \\ -\chi^{+*} & \xi^0 & \chi^+ \\ \chi^{++*} & \xi^- & \chi^0 \end{pmatrix} \quad (6.57)$$

where $\xi^- = -(\xi^+)^*$, which transform under $SU(2)_L \times SU(2)_R$ as $(\frac{1}{2}, \frac{1}{2})$ and $(1, 1)$ representations, respectively. The electroweak symmetry breaking preserves $SU(2)_c$ when the vevs of the fields are diagonal, $\langle \chi \rangle = v_\chi \mathbf{I}$ and $\langle \phi^0 \rangle = (v_\phi/\sqrt{2})\mathbf{I}$, where \mathbf{I} is the unit matrix. The vevs are constrained by the W mass to satisfy

$$v_{\text{SM}}^2 = v_\phi^2 + 8v_\chi^2. \quad (6.58)$$

It is convenient to parameterize the ratio of vevs by

$$\tan \theta_H \equiv \frac{2\sqrt{2}v_\chi}{v_\phi}. \quad (6.59)$$

Under the electroweak symmetry breaking, the $SU(2)_L \times SU(2)_R$ symmetry is broken down to $SU(2)_c$. A representation (T, T) of $SU(2)_L \times SU(2)_R$ decomposes into a set of representations of $SU(2)_c$, in particular, $2T \oplus 2T - 1 \oplus \dots \oplus 1 \oplus 0$. In the triplet G–M model, Φ breaks down to a triplet and a singlet of $SU(2)_c$, and χ breaks down to a five-plet, a triplet, and a singlet of $SU(2)_c$. The W^\pm and Z bosons are given mass by absorbing the $SU(2)_c$ triplet of Goldstone bosons,

$G_3^{+,0,-}$. The remaining physical states are a five-plet $H_5^{+,+,0,-,-}$, a triplet $H_3^{+,0,-}$, and two singlets H_1^0 and $H_1^{0'}$. If the Higgs potential is chosen to preserve $SU(2)_c$, then states transforming in different representations of $SU(2)_c$ cannot mix, and the states in each representation are degenerate. This model contains only one doublet Φ which gives mass to both the top- and bottom-type quarks. Therefore it is a Type I model and $\lambda_b \ll \lambda_t$. Thus the only sizeable correction to the $Zb\bar{b}$ vertex in this model will come from the left-handed charged Higgs boson loops.

The two singly-charged Higgs bosons and G^+ can be written in terms of the combinations of triplet fields

$$\psi^+ = \frac{1}{\sqrt{2}}(\chi^+ - \xi^+), \quad (6.60)$$

which transforms in a triplet of $SU(2)_c$, and

$$\zeta^+ = \frac{1}{\sqrt{2}}(\chi^+ + \xi^+), \quad (6.61)$$

which transforms in a five-plet of $SU(2)_c$. Then, the singly charged Higgs bosons are

$$G_3^+ = c_H \phi^+ + s_H \psi^+, \quad (6.62)$$

$$H_3^+ = -s_H \phi^+ + c_H \psi^+, \quad (6.63)$$

$$H_5^+ = \zeta^+, \quad (6.64)$$

where $s_H \equiv \sin \theta_H$ and $c_H \equiv \cos \theta_H$.

If the Higgs potential is chosen to preserve $SU(2)_c$ then H_3^+ and H_5^+ are mass eigenstates because they transform under different representations of $SU(2)_c$ [41]. Such a potential is desirable because it preserves $SU(2)_c$ (and $\rho = 1$) to all orders in the Higgs self-couplings. However, renormalization of the parameters in the Higgs potential at one loop introduces quadratically divergent terms that break $SU(2)_c$ [42]. These terms lead to quadratically divergent contributions to the ρ -parameter and to the mixing of some of the Higgs states, including H_3^+ and H_5^+ . In order to cancel the divergent corrections, $SU(2)_c$ -breaking counterterms must be introduced in the bare Lagrangian and fine-tuned to restore $\rho \simeq 1$. These $SU(2)_c$ -violating corrections arise at the two-loop level in R_b , so they will be neglected here.

The couplings in this model have been given in refs. [43,11]. They are also derived in ref. [24] for a general G-M model containing one multiplet $\Phi = (\frac{1}{2}, \frac{1}{2})$ and one larger multiplet $X = (T, T)$. The doublet field Φ is the only field with quark Yukawa couplings. Under $SU(2)_c$ the doublet decomposes into a singlet and a triplet. Thus only $SU(2)_c$ singlets and triplets can contain a doublet admixture and couple to quarks. This is a general feature of any model whose Higgs sector

obeys a custodial $SU(2)_c$ symmetry. In the triplet G–M model the charged Higgs couplings to quarks are

$$g_{G^+ \bar{t} b}^L = \frac{gm_t}{\sqrt{2}M_W}, \quad (6.65)$$

$$g_{H_3^+ \bar{t} b}^L = \frac{-gm_t}{\sqrt{2}M_W} \tan \theta_H, \quad (6.66)$$

$$g_{H_5^+ \bar{t} b}^L = 0. \quad (6.67)$$

These couplings also hold in a general G–M model containing $\Phi = (\frac{1}{2}, \frac{1}{2})$ and $X = (T, T)$, if $\tan \theta_H$ is defined as

$$\tan \theta_H = \frac{v_X \sqrt{\frac{4}{3}T(T+1)(2T+1)}}{v_\phi}, \quad (6.68)$$

where the vevs are constrained by the W mass to satisfy

$$v_{\text{SM}}^2 = v_\phi^2 + \frac{4}{3}T(T+1)(2T+1)v_X^2. \quad (6.69)$$

The loop corrections to R_b will only involve the charged Higgs states that appear in the triplet representations of $SU(2)_c$; namely, H_3^+ and G^+ .

The relevant ZH^+H^- couplings for charged Higgs bosons in a triplet of $SU(2)_c$ for any model which preserves $SU(2)_c$ are given below:

$$\begin{aligned} g_{ZG^+G^-} &= \frac{-e}{s_W c_W} \left(\frac{1}{2} - s_W^2 \right), \\ g_{ZG^+H_3^-} &= 0, \\ g_{ZH_3^+H_3^-} &= \frac{-e}{s_W c_W} \left(\frac{1}{2} - s_W^2 \right), \end{aligned} \quad (6.70)$$

as shown in ref. [24]. The loop corrections to R_b involving H^+ are particularly simple because the $ZG^+H_3^-$ coupling is zero.

In any model which preserves $SU(2)_c$ and contains only two multiplets Φ and X , the correction to δg^L is (not including the SM correction due to the charged Goldstone loops):

$$\delta g^L = \frac{1}{32\pi^2} \left(\frac{gm_t}{\sqrt{2}M_W} \right)^2 \tan^2 \theta_H \frac{e}{s_W c_W} \left[\frac{R}{R-1} - \frac{R \log R}{(R-1)^2} \right], \quad (6.71)$$

from loops involving H_3^+ , where $R \equiv m_t^2/M_{H_3^+}^2$. This correction is positive definite and has the same form as the correction in the 2HDM (equation 6.2).

In general for a model with custodial $SU(2)_c$ and more than one exotic multiplet X , the correction becomes

$$\delta g^L = \frac{1}{32\pi^2} \sum_{H_{3i}^+} (g_{H_{3i}^+ \bar{t} b}^L)^2 \frac{e}{s_W c_W} \left[\frac{R_i}{R_i - 1} - \frac{R_i \log R_i}{(R_i - 1)^2} \right], \quad (6.72)$$

which is positive definite. Thus when the Higgs potential is invariant under $SU(2)_c$, the corrections always decrease R_b .

As in the 2HDM, the R_b measurement can be used to set a lower bound on the mass of the $SU(2)_c$ triplet H_3 , which varies with $\tan \theta_H$. This bound is independent of the isospin of the exotic $SU(2)_L \times SU(2)_R$ multiplet X (or χ in the triplet G–M model). In fig. 11 we plot the bound on M_{H_3} as a function of $\tan \theta_H$.

For H_3 lighter than about 1 TeV, the R_b measurement implies that $\tan \theta_H < 2$. In the triplet G–M model, this corresponds to an upper limit on the triplet vev of $v_\chi/v_\phi < 0.7$. As in the Type I 2HDM, the charged Higgs boson contribution to $b \rightarrow s\gamma$ is small compared to the contribution in the Type II 2HDM [44], and the $b \rightarrow s\gamma$ measurement does not provide additional bounds on the parameter space. In contrast, for the parameter regions considered above, the correction to A_b is negligible ($|\Delta A_b| < 0.002$) compared to the experimental uncertainty in the A_b measurement.

Higgs potential without $SU(2)_c$ invariance If the requirement of $SU(2)_c$ symmetry is relaxed, it is no longer meaningful to write the Higgs fields with $SU(2)_L \times SU(2)_R$ matrices. In the triplet model we must define the vevs of the two $SU(2)_L$ triplets separately, $\langle \chi^0 \rangle = v_\chi$, and $\langle \xi^0 \rangle = v_\xi$. Then $SU(2)_c$ symmetry corresponds to $v_\chi = v_\xi$. The triplet model can still satisfy $\rho = 1$ if the Higgs potential is fine-tuned so that $v_\chi = v_\xi$. In this situation the two physical charged Higgs bosons H_3^+ and H_5^+ can mix with each other. If we parameterize this mixing with an angle α , the new mass eigenstates are

$$\begin{aligned} H_1^+ &= \sin \alpha H_3^+ + \cos \alpha H_5^+, \\ H_2^+ &= \cos \alpha H_3^+ - \sin \alpha H_5^+. \end{aligned} \quad (6.73)$$

The charged Higgs couplings to the Z and quark pairs are

$$\begin{aligned} g_{H_1^+ \bar{t} b}^L &= \frac{g m_t}{\sqrt{2} M_W} \tan \theta_H \sin \alpha, \\ g_{H_2^+ \bar{t} b}^L &= \frac{g m_t}{\sqrt{2} M_W} \tan \theta_H \cos \alpha, \\ g_{ZG^+ H_1^-} &= \frac{-e}{s_W c_W} \frac{1}{2} s_H \cos \alpha, \\ g_{ZG^+ H_2^-} &= \frac{e}{s_W c_W} \frac{1}{2} s_H \sin \alpha, \end{aligned}$$

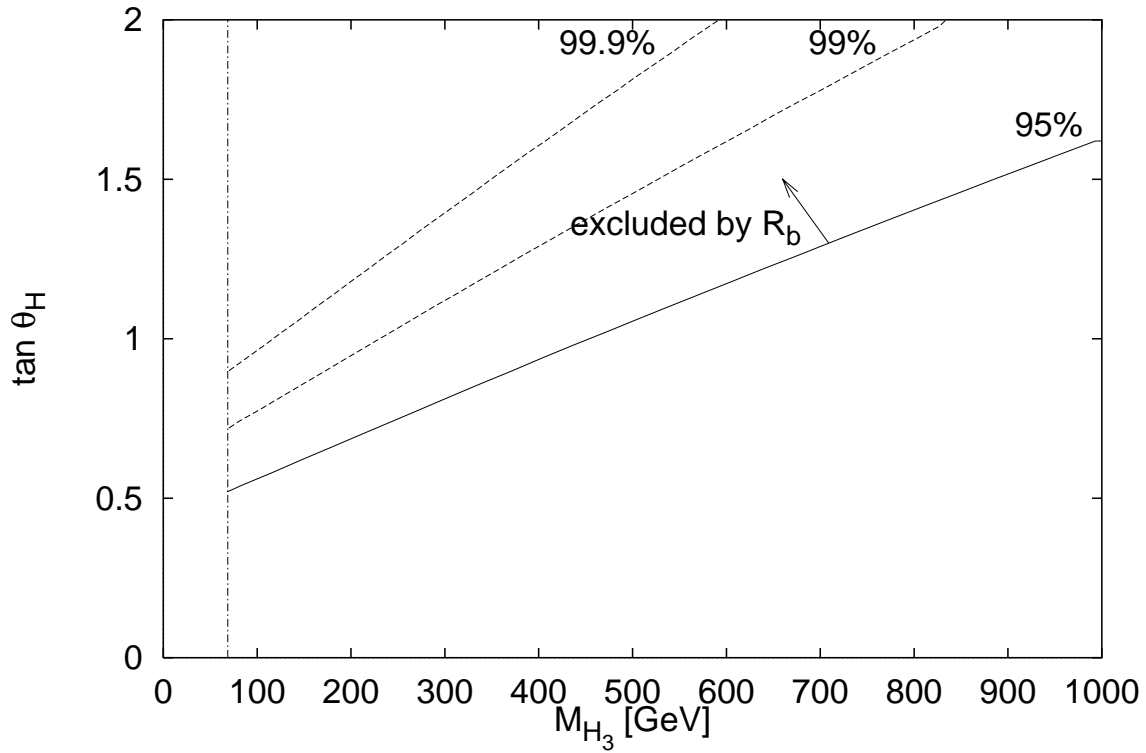


Fig. 11. Bounds from R_b for the G–M model with Higgs triplets and $SU(2)_c$ symmetry. The area above the solid line is ruled out at 95% confidence level by R_b . Also shown (top to bottom) are the 99.9% and 99% confidence level contours (dashed). The dot-dashed line corresponds to the LEP lower limit for the H^+ mass, $M_{H^+} > 77.3$ GeV [37].

$$\begin{aligned}
g_{ZH_1^+ H_1^-} &= \frac{-e}{s_W c_W} \left(\frac{1}{2} - s_W^2 - c_H \sin \alpha \cos \alpha \right), \\
g_{ZH_1^+ H_2^-} &= \frac{-e}{s_W c_W} \frac{1}{2} c_H (\sin^2 \alpha - \cos^2 \alpha), \\
g_{ZH_2^+ H_2^-} &= \frac{-e}{s_W c_W} \left(\frac{1}{2} - s_W^2 + c_H \sin \alpha \cos \alpha \right).
\end{aligned} \tag{6.74}$$

Both of the singly charged Higgs bosons couple to quarks instead of just one. There are now off-diagonal $ZH_i^+ H_j^-$ couplings with $i \neq j$ and non-SM-like terms in the diagonal couplings which contribute to δg^L . We find:

$$\begin{aligned}
\delta g_{H^+}^L &= \delta g_{G^+}^L (\text{SM}) \\
&+ \frac{1}{32\pi^2} \frac{e}{s_W c_W} \left(\frac{gm_t}{\sqrt{2}M_W} \right)^2 \tan^2 \theta_H \\
&\quad \times \left\{ \sin^2 \alpha \left[\frac{R_1}{R_1 - 1} - \frac{R_1 \log R_1}{(R_1 - 1)^2} \right] + \cos^2 \alpha \left[\frac{R_2}{R_2 - 1} - \frac{R_2 \log R_2}{(R_2 - 1)^2} \right] \right\} \\
&+ \frac{1}{16\pi^2} \left(\frac{e}{s_W c_W} \right) \left(\frac{gm_t}{\sqrt{2}M_W} \right)^2 \tan^2 \theta_H (2c_H \sin \alpha \cos \alpha) \\
&\quad \times \left\{ C_{24}(m_t^2, M_W^2, M_2^2) - C_{24}(m_t^2, M_W^2, M_1^2) \right. \\
&\quad + \sin^2 \alpha [C_{24}(m_t^2, M_1^2, M_1^2) - C_{24}(m_t^2, M_1^2, M_2^2)] \\
&\quad \left. + \cos^2 \alpha [C_{24}(m_t^2, M_1^2, M_2^2) - C_{24}(m_t^2, M_2^2, M_2^2)] \right\},
\end{aligned} \tag{6.75}$$

where $R_i \equiv m_i^2/M_i^2$. The first term is the SM correction due to G^+ . The second term is positive definite and has the same mass dependence as the charged Higgs boson correction in the 2HDM. The third term arises from the off-diagonal $ZH^+ H^-$ couplings and the non-SM parts of the diagonal $ZH^+ H^-$ couplings. This third term can be positive or negative, depending on the mixing angle α . It is negative for $M_{H_2^+} > M_{H_1^+}$ when $\sin \alpha \cos \alpha$ is positive, and grows with increasing splitting between $M_{H_1^+}$ and $M_{H_2^+}$ and between M_W and the charged Higgs masses.

This model is fine-tuned to $v_\chi = v_\xi$ to give $\rho = 1$; when the parameters of the Higgs potential are renormalized this fine-tuning will be lost. In order to satisfy the experimental bounds on $\Delta\rho_{\text{new}}$ [eq. (6.35)], we must have

$$-1.7 \times 10^{-3} < \Delta\rho_{\text{new}} = \frac{4(v_\xi^2 - v_\chi^2)}{v_\phi^2 + 8v_\chi^2} < 2.7 \times 10^{-3} \tag{6.76}$$

or $-(5.1 \text{ GeV})^2 < v_\xi^2 - v_\chi^2 < (6.4 \text{ GeV})^2$. For the model to be ‘‘natural’’ we require the parameters to be of the same order as their fine-tuning, or $v_\chi \sim v_\xi \sim 6 \text{ GeV}$. Then the correction to the SM result in eq. (6.75) is suppressed by a factor of $\tan^2 \theta_H \sim 0.005$.

7 Conclusions

Radiative corrections to the process $Z \rightarrow b\bar{b}$ arise in extended Higgs sectors due to the exchange of the additional singly-charged and neutral Higgs bosons. Because the radiative corrections affect the predictions for R_b and A_b , the measurements of these quantities can in principle be used to constrain the parameter space of the models. The radiative corrections to R_b from extended Higgs sectors are typically of the same order of magnitude as the experimental error in the R_b measurement. Thus R_b can be used to constrain the models. However, the radiative corrections to A_b from extended Higgs sectors are much smaller than the experimental error in the A_b measurement. They are also much smaller than the deviation of the A_b measurement from the SM prediction. We conclude that if $A_b \neq A_b^{\text{SM}}$, the deviation does not arise from the contributions of an extended Higgs sector.

In this paper we obtained general formulae for the corrections to the $Zb\bar{b}$ vertex, and then used the general formulae to calculate the contributions to R_b and A_b in specific models. Here we summarize our conclusions for the various models.

The contributions from neutral Higgs boson exchange are only significant in a Type II model with enhanced λ_b . The regions of parameter space in which the contribution to R_b from neutral Higgs boson exchange can be positive is nearly ruled out by direct Higgs boson searches. Otherwise, the contribution to R_b is negative, giving a worse agreement with experiment than the SM. A pair of neutral Higgs states, H^0 and A^0 , with a significant ZH^0A^0 coupling and a large mass splitting, gives a large negative contribution to R_b . The R_b measurement can then be used to exclude these regions of parameter space.

The contributions to R_b from charged Higgs boson exchange are negative in models which contain only doublets and singlets, and in any model whose Higgs sector preserves $SU(2)_c$ symmetry. If the contributions from neutral Higgs boson exchange in these models are not significant (*e.g.*, if λ_b is small), then R_b sets a lower bound on the masses of the charged Higgs states. The lower bound depends on λ_t and the charged Higgs mixing angles.

The contribution to R_b from charged Higgs boson exchange can only be positive if the model contains one of two features. It must either contain off-diagonal $ZH_i^+H_j^-$ couplings in which both of the charged Higgs bosons couple to quarks and have different masses, or it must contain diagonal $ZH_i^+H_i^-$ couplings which differ from the couplings in doublet models, or both. This can only happen in models which contain Higgs multiplets larger than doublets and are not constrained by $SU(2)_c$ symmetry. In such a model, the vevs of the multiplets larger than doublets must be very small in order for the model to be consistent with the measured value of the ρ parameter. With this constraint, the contribution to R_b can only be positive when the model contains more than one doublet and there is significant mixing between the doublets and the larger multiplets.

The precision of the R_b and A_b measurements is not likely to improve significantly in the near future. Most of the LEP and SLC Z pole data has been analyzed, and no further running of these machines at $\sqrt{s} = M_Z$ is anticipated. Thus, future constraints on extended Higgs sectors must come from other sources. New virtual constraints on extended Higgs sectors will come from measurements of b quark decays at the high-luminosity B -factories which will soon be sensitive to a variety of rare B decay modes. For example, the processes $b \rightarrow s\ell^+\ell^-$ and $b \rightarrow s\gamma$ are sensitive to the virtual charged-Higgs exchange (the latter process has already been used to constrain the extended Higgs parameter space). In addition, the process $b \rightarrow s\tau^+\tau^-$ receives a contribution from a neutral Higgs boson coupled to the $\tau^+\tau^-$ pair, whereas $b \rightarrow c\tau\nu$ receives a contribution from tree-level charged Higgs boson exchange [45,46,47]. High statistics samples of these decay modes will yield interesting new constraints on the structure of the extended Higgs sector.

Ultimately, one will need to directly probe the extended Higgs sector by explicitly producing the scalar states (beyond h^0 which may resemble the SM Higgs boson) at future colliders. If some signal is seen, it will be a demanding task to interpret the signal and deduce the structure of the underlying scalar sector. The constraints on the Higgs sector parameter space from R_b and other rare B decay modes can play an important role in helping to unravel the physics of the Higgs sector and probe the origin of electroweak symmetry breaking.

A Contribution to the ρ parameter in the 2HDM

In this appendix we give the one-loop contribution of the Higgs bosons in the 2HDM to the ρ parameter, from ref. [48]:⁵

$$\begin{aligned} \Delta\rho = \frac{\alpha}{16\pi M_W^2 s_W^2} & \left\{ F(M_{H^\pm}^2, M_{A^0}^2) + \sin^2(\beta - \alpha) \left[F(M_{H^\pm}^2, M_{H^0}^2) - F(M_{A^0}^2, M_{H^0}^2) \right] \right. \\ & + \cos^2(\beta - \alpha) \left[F(M_{H^\pm}^2, M_{h^0}^2) - F(M_{A^0}^2, M_{h^0}^2) + F(M_W^2, M_{H^0}^2) \right. \\ & \quad - F(M_W^2, M_{h^0}^2) - F(M_Z^2, M_{H^0}^2) + F(M_Z^2, M_{h^0}^2) \\ & \quad + 4M_Z^2 \left[B_0(0; M_Z^2, M_{H^0}^2) - B_0(0; M_Z^2, M_{h^0}^2) \right] \\ & \quad \left. \left. - 4M_W^2 \left[B_0(0; M_W^2, M_{H^0}^2) - B_0(0; M_W^2, M_{h^0}^2) \right] \right] \right\} \quad (\text{A.1}) \end{aligned}$$

⁵A typographical error in the formula for $\Delta\rho$ in ref. [48] is corrected in eq. (A.1).

where $s_W \equiv \sin \theta_W$, and

$$B_0(0; m_1^2, m_2^2) = \frac{A_0(m_1^2) - A_0(m_2^2)}{m_1^2 - m_2^2} \quad (\text{A.2})$$

$$A_0(m^2) \equiv m^2[\Delta + 1 - \log(m^2/\mu^2)] \quad (\text{A.3})$$

$$F(m_1^2, m_2^2) \equiv \frac{1}{2}(m_1^2 + m_2^2) - \frac{m_1^2 m_2^2}{m_1^2 - m_2^2} \log\left(\frac{m_1^2}{m_2^2}\right). \quad (\text{A.4})$$

We have defined $\Delta\rho$ relative to the SM where the SM Higgs mass is taken equal to M_{h^0} . With this definition, $\Delta\rho$ is a finite quantity and is independent of the scale, μ , and the divergence, $\Delta \equiv 1/\epsilon - \gamma + \log(4\pi)$, of dimensional regularization.

B Constraints from direct Higgs searches

In this appendix, we briefly summarize the constraints on extended Higgs sectors resulting from the direct Higgs searches at LEP.

B.1 Charged Higgs searches

At LEP, charged Higgs bosons are produced via $e^+e^- \rightarrow \gamma^*, Z^* \rightarrow H^+H^-$. The LEP analysis then assumes that $\text{BR}(H^+ \rightarrow c\bar{s}) + \text{BR}(H^+ \rightarrow \tau^+\nu_\tau) \simeq 1$. The resulting limit obtained in ref. [37] is $M_{H^+} > 77.3$ GeV. This mass limit would be relaxed if other charged Higgs decay modes are significant. In extended Higgs models with two or more singly-charged Higgs bosons, we shall apply the LEP bound only to the lightest charged Higgs state.

The LEP bound also depends on the production cross section of the charged Higgs boson pair. In the analysis of ref. [37] it is assumed that the ZH^+H^- coupling is that of the 2HDM:

$$g_{ZH^+H^-} = -\frac{e}{s_W c_W} \left(\frac{1}{2} - s_W^2\right). \quad (\text{B.1})$$

This coupling, and hence the resulting H^+H^- production cross section, is the same as the one that arises in models containing multiple doublets and singlets, and in the G–M models for H_3^\pm . The LEP charged Higgs mass bound is used for these models in figs. 5, 9 and 11. However, eq. (B.1) is *not* the same as the ZH^+H^- coupling that occurs in models containing doublets and triplets without $\text{SU}(2)_c$ symmetry. In models with one or two doublets and one real, $Y = 0$ triplet, the ZH^+H^- coupling is larger than in the 2HDM, and hence the production cross section is larger. Therefore in these models, the charged Higgs mass bound from ref. [37] is a conservative bound. This bound is used in fig. 9 for the model with

two doublets and one $Y = 0$ triplet. In models with one or two doublets and one complex, $Y = 2$ triplet, the coupling is smaller than in the 2HDM. Hence the charged Higgs boson production cross section is smaller, and the LEP charged Higgs mass bound is no longer valid. This is the case in fig. 10, for the model with two doublets and one $Y = 2$ triplet.

B.2 Neutral Higgs searches in the 2HDM

The search for neutral Higgs bosons at LEP focuses primarily on the SM Higgs boson and Higgs bosons of the Minimal Supersymmetric Model (MSSM). The SM Higgs boson is produced via $e^+e^- \rightarrow Z^* \rightarrow Zh^0$. In the MSSM, in addition to Zh^0 production, one can produce a CP-even Higgs boson in association with a CP-odd Higgs boson via $e^+e^- \rightarrow Z^* \rightarrow h^0A^0$. The MSSM Higgs sector is a 2HDM with particular relations among Higgs sector parameters. Thus, the MSSM Higgs mass bounds do not immediately apply to the general 2HDM.

From the combined LEP data taken at $\sqrt{s} = 189$ GeV, the lower limit on the SM Higgs mass obtained in ref. [37] is $M_{h_{\text{SM}}^0} > 95.2$ GeV. This bound depends primarily on the cross-section for $e^+e^- \rightarrow Z^* \rightarrow Zh^0$ (under the assumption that the decay branching fractions of the h^0 follow roughly the pattern expected in the SM). In the 2HDM, the ZZh^0 coupling is reduced from its SM value by a factor of $\sin(\beta - \alpha)$, resulting in

$$\sigma(e^+e^- \rightarrow Zh^0) = \sigma_{\text{SM}}(e^+e^- \rightarrow Zh^0) \sin^2(\beta - \alpha). \quad (\text{B.2})$$

The LEP bound on M_{h^0} in the SM is determined by the mass value at which $\sigma_{\text{SM}}(e^+e^- \rightarrow Zh^0)$ crosses the measured upper bound of $\sigma(e^+e^- \rightarrow Zh^0)$. Using eq. (B.2), this can then be translated into a bound on $\sin^2(\beta - \alpha)$ as a function of M_{h^0} . The resulting bound can be found in fig. 4 of ref. [37]. For $\sin^2(\beta - \alpha) = 1$, the bound on M_{h^0} is the same as in the SM, $M_{h^0} > 95.2$ GeV. This bound is used in fig. 8. For $\sin^2(\beta - \alpha) = 1/2$, the bound on M_{h^0} is $M_{h^0} \gtrsim 90$ GeV.⁶

In the above discussion, only the Zh^0 mode was considered. For a complete determination of the 2HDM parameter constraints, it is necessary to include the LEP limits on h^0A^0 (and H^0A^0) associated production via virtual s -channel Z -exchange. The Zh^0A^0 [ZH^0A^0] coupling is proportional to $\cos(\beta - \alpha)$ [$\sin(\beta - \alpha)$], so for fixed $\sin(\beta - \alpha)$ one can deduce a region in the M_{A^0} vs. M_{h^0} plane that is excluded by LEP data. Unfortunately, the LEP neutral Higgs boson search data are typically presented in the context of the MSSM, where Higgs sector parameters are correlated.⁷ For example, at large $\tan\beta$ and values of $M_{A^0} \lesssim M_Z$, one finds

⁶In fig. 6, a bound of $M_{h^0} > 87$ GeV is used, corresponding to our best estimate based on LEP data prior to the availability of fig. 4 of ref. [37].

⁷A more general 2HDM analysis has recently been presented by the OPAL Collaboration [49]. The results of this work came too late to be included in the analysis of this paper, although we expect only minor changes to our results.

that $M_{h^0} \approx M_{A^0}$ and $\cos(\beta - \alpha) \simeq 1$. This implies that in this region of MSSM parameter space, the LEP search is sensitive only to $h^0 A^0$ production.

To extract general 2HDM constraints, we proceed as follows. From the LEP search for $e^+e^- \rightarrow h^0 A^0$, the LEP MSSM analysis [37] yields $M_{h^0} > 80.7$ GeV and $M_{A^0} > 80.9$ GeV. These lower bounds correspond roughly to pure $h^0 A^0$ production at large $\tan\beta$. We can convert this into an upper limit for the $h^0 A^0$ cross-section for Higgs mass values at the respective lower bounds. To get results that apply more generally to the 2HDM (where M_{h^0} , M_{A^0} and $\cos(\beta - \alpha)$ are not correlated), we make the simplifying assumption that the Higgs boson detection efficiency and background is fairly flat as a function of the Higgs masses. We can then vary M_{h^0} and $\cos^2(\beta - \alpha)$ and find a lower bound on M_{A^0} .⁸ The resulting ‘‘direct search’’ bounds have been implemented in figs. 6 and 7. Further details of this analysis can be found in ref. [24].

References

1. R. Clare, talk presented at the 1999 American Physical Society Centennial Meeting, Atlanta, USA, 20–26 March 1999.
2. J. Mnich, talk presented at the 1999 International Europhysics Conference on High Energy Physics, Tampere, Finland, 15–21 July 1999.
3. M. Swartz, talk presented at the 1999 Lepton Photon Symposium, Stanford, CA, USA, 9–14 August 1999.
4. P. Sikivie, L. Susskind, M. Voloshin and V. Zakharov, *Nucl. Phys.* **B173**, 189 (1980).
5. J. Erler, hep-ph/9903449, talk presented at the Division of Particles and Fields Conference (DPF 99), Los Angeles, CA, 5–9 January 1999; P. Langacker, hep-ph/9905428, talk presented at the 17th International Workshop on Weak Interactions and Neutrinos (WIN 99), Cape Town, South Africa, 24–30 January, 1999.
6. A.A. Akhundov, D.Y. Bardin and T. Riemann, *Nucl. Phys.* **B276**, 1 (1986).
7. W. Beenakker and W. Hollik, *Z. Phys.* **C40**, 141 (1988).
8. J. Bernabeu, A. Pich and A. Santamaria, *Phys. Lett.* **B200**, 569 (1988).
9. W. Hollik, *Fortschr. Phys.* **38**, 165 (1990).
10. B.W. Lynn and R.G. Stuart, *Phys. Lett.* **B252**, 676 (1990).
11. J.F. Gunion, H.E. Haber, G.L. Kane and S. Dawson, *The Higgs Hunter’s Guide* (Addison-Wesley Publishing Company, Redwood City, CA, 1990).
12. S.L. Glashow and S. Weinberg, *Phys. Rev.* **D15**, 1958 (1977).
13. E.A. Paschos, *Phys. Rev.* **D15**, 1966 (1977).
14. D. Atwood, L. Reina and A. Soni, *Phys. Rev.* **D55**, 3156 (1997).
15. H.E. Haber and Y. Nir, *Nucl. Phys.* **B335**, 363 (1990).

⁸For $|\cos(\beta - \alpha)| \ll 1$, the production of $H^0 A^0$ rather than $h^0 A^0$ is relevant.

16. A. Kundu and B. Mukhopadhyaya, *Int. J. Mod. Phys.* **A11**, 5221 (1996).
17. A. Denner, R.J. Guth, W. Hollik and J.H. Kuhn, *Z. Phys.* **C51**, 695 (1991).
18. A. Djouadi *et al.*, *Nucl. Phys.* **B349**, 48 (1991).
19. M. Bouwens and D. Finnell, *Phys. Rev.* **D44**, 2054 (1991).
20. A.K. Grant, *Phys. Rev.* **D51**, 207 (1995).
21. R. Barbieri and G.F. Giudice, *Phys. Lett.* **B301**, 358 (1993).
22. H.E. Haber, in *Properties of SUSY Particles*, Proceedings of the 23rd Workshop of the INFN Eloisatron Project, Erice, Italy, September 28–October 4, 1992, edited by L. Cifarelli and V.A. Khoze (World Scientific, Singapore, 1993) p. 321.
23. A. Dobado, M.J. Herrero and S. Penaranda, *Eur. Phys. J.* **C7**, 313 (1999); hep-ph/9903211 (*Eur. Phys. J. C*, in press).
24. H.E. Logan, Ph.D. thesis, U.C. Santa Cruz, 1999, SCIPP 99/25, hep-ph/9906332.
25. J. Field, *Mod. Phys. Lett.* **A13**, 1937 (1998).
26. H. Fusaoka and Y. Koide, *Phys. Rev.* **D57**, 3986 (1998).
27. D. Abbaneo *et al.* [ALEPH, DELPHI, L3, OPAL, LEP Electroweak Working Group, and SLD Heavy Flavour and Electroweak Groups], CERN-EP/99-15.
28. M.E. Peskin and T. Takeuchi, *Phys. Rev. Lett.* **65**, 964 (1990); *Phys. Rev.* **D46**, 381 (1992).
29. A.K. Grant and T. Takeuchi, hep-ph/9807413.
30. C. Caso *et al.*, *Eur. Phys. J.* **C3**, 1 (1998).
31. H.-S. Tsao, in *Proceedings of the 1980 Guangzhou Conference on Theoretical Particle Physics*, edited by H. Ning and T. Hung-yuan (Science Press, Beijing, 1980), p. 1240.
32. W. Hollik, in *Precision Tests of the Standard Electroweak Model*, edited by P. Langacker (World Scientific, Singapore, 1995), p. 117.
33. W. Hollik, in *Precision Tests of the Standard Electroweak Model*, edited by P. Langacker (World Scientific, Singapore, 1995), p. 37.
34. M.C. Peyranere, H.E. Haber and P. Irulegui, *Phys. Rev.* **D44**, 191 (1991).
35. S. Ahmed *et al.* [CLEO Collaboration], CLEO CONF 99-10, hep-ex/9908022.
36. F.M. Borzumati and C. Greub, *Phys. Rev.* **D58**, 074004 (1998); **D59**, 057501 (1999).
37. P. Bock *et al.* [ALEPH, DELPHI, L3 and OPAL Collaborations; The LEP working group for Higgs boson searches], ALEPH 99-081 CONF 99-052, DELPHI 99-142 CONF 327, L3 Note 2442, and OPAL Technical Note TN-614, submitted to the International Europhysics Conference on High Energy Physics, 15–21 July 1999, Tampere, Finland.
38. B. Abbott *et al.* [D0 Collaboration], *Phys. Rev. Lett.* **82**, 4975 (1999).
39. H.E. Haber, in Proceedings of the US–Polish Workshop, Warsaw, Poland, September 21–24, 1994, edited by P. Nath, T. Taylor, and S. Pokorski (World Scientific, Singapore, 1995) p. 49.

40. H. Georgi and M. Machacek, *Nucl. Phys.* **B262**, 463 (1985).
41. M.S. Chanowitz and M. Golden, *Phys. Lett.* **165B**, 105 (1985).
42. J.F. Gunion, R. Vega and J. Wudka, *Phys. Rev.* **D43**, 2322 (1991).
43. J.F. Gunion, R. Vega and J. Wudka, *Phys. Rev.* **D42**, 1673 (1990).
44. B. Grinstein, R. Springer and M.B. Wise, *Nucl. Phys.* **B339**, 269 (1990).
45. P. Krawczyk and S. Pokorski, *Phys. Rev. Lett.* **60**, 182 (1988).
46. J. Kalinowski, *Phys. Lett.* **B245**, 201 (1990).
47. Y. Grossman and Z. Ligeti, *Phys. Lett.* **B332**, 373 (1994).
48. H.E. Haber, in *Perspectives on Higgs Physics*, edited by G.L. Kane (World Scientific, Singapore, 1993), p. 79.
49. The OPAL Collaboration, OPAL Physics Note PN-416 (August 11, 1999).